Bridging blood cancers and inflammation

The reduced Cancitis model

Ottesen, Johnny T.; Pedersen, Rasmus Kristoffer; Sajid, Zamra; Gudmand-Høyer, Johanne; Bangsgaard, Katrine O.; Skov, Vibe; Kjær, Lasse; Knudsen, Trine A.; Pallisgaard, Niels; Hasselbalch, Hans; Wienecke Andersen, Morten

Bridging blood cancers and inflammation: the reduced Cancitis model

Johnny T. Ottesen[1]* Rasmus K. Pedersen[1], Zamra Sajid[1],
Johanne Gudmand-Hoeyer[1], Katrine O. Bangsgaard[1], Vibe Skov[2],
Lasse Kjær[2], Trine Alma Knudsen[2], Niels Pallisgaard[2],
Hans C. Hasselbalch[2], & Morten Andersen[1],

[1]Department of Science and Environment, Roskilde University, Denmark.

[2]Department of Hematology, Zealand University Hospital, University of Copenhagen, Denmark.

*Corresponding author, Johnny@ruc.dk

Abstract

A novel mechanism-based model - the Cancitis model - describing the interaction of blood cancer and the inflammatory system is proposed, analyzed and validated. The immune response is divided into two components, one where the elimination rate of malignant stem cells is independent of the level of the blood cancer and one where the elimination rate depends on the level of the blood cancer. A dimensional analysis shows that the full 6-dimensional system of nonlinear ordinary differential equations may be reduced to a 2-dimensional system - the reduced Cancitis model - using Fenichel theory. The original 18 parameters appear in the reduced model in 8 groups of parameters. The reduced model is analyzed. Especially the steady states and their dependence on the exogenous inflammatory stimuli are analyzed. A semi-analytic investigation reveals the stability properties of the steady states. Finally, positivity of the system and the existence of an attracting trapping region in the positive octahedron guaranteeing global existence and uniqueness of solutions are proved. The possible topologies of the dynamical system are completely determined as having a Janus structure, where two qualitatively different topologies appear for different sets of parameters. To classify this Janus structure we propose a novel concept in blood cancer - a reproduction ratio $\mathcal{R}$. It determines the topological structure depending on whether it is larger or smaller than a threshold value. Furthermore, it follows that inflammation, affected by the exogenous inflammatory stimulation, may determine the onset and development of blood cancers. The body may manage initial blood cancer as long as the self-renewal rate is not too high, but fails to manage it if an inflammation appears. Thus, inflammation may trigger and drive blood cancers. Finally, the mathematical analysis suggests novel treatment strategies and it is used to discuss the *in silico* effect of existing treatment, e.g. interferon-α or T-cell therapy, and the impact of malignant cells becoming resistant.

1. Introduction

Formation of blood cells, hematopoiesis, takes place in the bone marrow by cell division of hematopoietic stem cells (HSCs). Mutations of HSCs

may lead to cancerous stem cells causing blood cancers, which ultimatively suppress production of healthy blood cells [13, 21]. The myeloproliferative neoplasms (MPNs) are disorders emanating from the bone marrow and predominantly consisting of chronic myelogeneous leukemia (CML), essential thrombocythemia (ET), polycythemia vera (PV), and primary myelofibrosis (PMF) [11]. Despite similarities, common theoretical considerations can be applied, since the diseases share clonal hematopoiesis as a hallmark and are strongly influenced by - and coupled with - the inflammatory response of the immune system [19].

In this article we develop a model of the system underlying the blood cancer diseases coupled to the inflammatory response system. The model presented in [2] is used as a starting point and only what is truly important for the purpose af the model is included.

Most cancers are developed somewhat similarly in the early avascular phase before tumor size plays a role [70, 71]. Thus, the present model may be adapted for early cancer more generally despite it being developed specifically for blood cancers. Some blood cancers are curable, while others, such as MPNs, are more challenging [61, 1]. Thus, special attention will be on MPNs although the frequency of getting MPNs is relatively low.

In [2] a novel and mechanism-based model of blood cancers coupled to the inflammatory response of the immune system was proposed. The model is to our knowledge the first of its kind and furthermore generic in the sense that it describes blood cancer in general. Shortly after, Komarova et. al. published a simplified approach to discuss the role of inflammation in MPNs [72]. They include stem cell dynamics and bone marrow niche feedback, but describe the inflammation as a fixed parameter independent of the actual cancer development, i.e. independent of the immune response to the cancer cells. This approach is somewhat similar to the 2-dimensional approach taken in [24], where a simple model of stem cell dynamics including bone marrow niche feedback, but without including inflammation, was investigated.

In [2] T-cells were not explicitly considered, but in the present study we include the effect of these. Accumulated evidence has indicated that the immune system may recognize and eliminate malignant cells [52, 60] acting as a control mechanism for maintaining homeostasis. This effect is called immune surveillance, a concept attributed to Thomas and MacFarlane in the late 1950s although a similar idea was promoted by Ehrlich already in 1909. Today it is refined into the concept of immunoediting [55].

An early mathematical model describing interaction of tumor cells and effector cells (killer cells) for BCL1 lymphoma was presented by Kuznetsov and Knott [41] continuing the work from [42], and was based on a logistic growth equation to describe the intrinsic dynamics. Several models of the role of inflammation in general cancer progression have since been studied.

Most of these modeling attempts consider solid tumors and couples the T-cell and natural killer (NK) cell dynamics to a logistic growth description of tumors. The models in [54, 18, 53, 59, 17, 8, 34, 58, 28, 50, 51, 4, 32, 23, 3, 36, 5, 6, 48, 49] are simplified models describing how solid cancers may stimulate the T-cells dynamics, while the cancer dynamics are decoupled from the rest of the system, simply described as logistic growth or similar. The works by Kuznetsov and Knott, Moore, Zhang et. al., Nanda et. al. [41, 72, 48, 49] and the excellent books by Wodarz and Komarova [71, 38] point toward the direction taken in the present paper.

Clapp et al (2015) [15] consider a 5D model including active and quiescent stem cells, progenitor cells, mature cells and one immune compartment to describe chronic myelogenous leukemia. The active stem cell pool is based on the logistic growth equation omitting interactions with the normal hematopoietic cells. Recently Besse et. al. (2018) [7] investigate a simplified version of this model. Simultaneously Talkington et. al. (2018) [65] compared four models of acute lymphocytic leukemia, namely those by Kuznetsov et. al (1994) [42], Kirschner and Panetta (1998) [36], Dong et. al. (2014) [22], and Moore and Li (2004) [48]. The purpose was to study modified T-cells engineered to recognize CD19 surface marker clinically, resulting in partial success in virtual treatment of the disease. All four models predict a positive effect of the treatment. Historically, a few important models addressing tyrosine kinase inhibitors (TKI), e.g. imatinib, in treating chronic myelogenous leukemia have appeared. Michor et. al. (2005) [46] explained incomplete eradication of CML under TKI treatment by resistance. Komarova and Wodarz (2007) [37] incorporated quiescent stem cells and the development of resistance to treatment. Using an agent-based model, Roeder et al. (2006) [57] describe competition between leukemic stem cells and normal hematopoietic stem cells and included the effect of TKIs on the competition. Long-term effect of the immune response was modeled by Kim et al. (2008) [35] by adding an unspecific immune component to the model by Michor et al. (2005) [46].

Recently, Brady et. al. [9] suggested an inflammatory model coupled to the autonomic regulation of the cardiovascular system for healthy subjects exposed to intravenous injection of lipopolysaccharide (LPS) to stimulate an inflammatory response. Simultaneously, Bangsgaard et. al. [6] suggested a detailed inflammatory response model coupled to the Hypothalamic–Pituitary–Adrenal axis allowing an exogeneous stimuli. This so-called ITIS model contains eight time-dependent variables: Endotoxin, phagocytic cells, pro- and anti-inflammatory cytokines (a broad category of signaling molecules consisting of small proteins): TNF-α, IL-10, TGF-β, CRH, ACTH and cortisol. The ITIS model is capable of reproducing available data and has served as an inspiration in the present work, but in a suitable simplified form.

The outline of the paper is as follows. In section 2 the model is presented and in subsection 2.1 it is expanded by explicitly including a description of the interaction with immune response effector cells such as T-cells. The model is put on a dimensionless form and based on a separation of time scales, a two-dimensional model - the reduced Cancitis model - is suggested in section 3. The reduced Cancitis model is analyzed in section 4. Admissible steady states are derived and in subsection 4.1 their stability properties are examined depending on the external inflammatory stimuli. A complete analysis of the topology of the dynamical system is presented, showing a Janus topology[1]. An attracting trapping region is constructed in subsection 4.2 establishing global existence and uniqueness of solutions. A treatment plan by T-cell gene therapy appear in subsection 4.3 along with a description of how the phase plane varies with increasing external inflammatory stimuli. Special focus is on the role of the level of external inflammatory stimuli and its effect on existence and stability of healthy and unhealthy steady states of the model. The various findings are discussed and conclusions made in section 5. Finally, some cumbersome derivations related to the steady states are presented in Appendix A and Appendix B.

2. The model

As in the previous model presented in [2] focus will be on ensembles of each cell type and not the individual cells. Hence, the governing laws will be for the pools of cells, commonly denoted compartments. The compartments encompass the healthy hematopoietic stem cells in the bone marrow, the healthy hematopoietic mature cells in the blood, the malignant stem cells in the bone marrow, the malignant mature cells in blood, the pool of dead cells and the resulting debris not yet cleared, and a variable describing the immune system activity level, which correlates with the associated cytokines related to the disease. In what follows we will denote healthy hematopoietic cells shortly as hematopoietic cells in contrast to e.g. malignant cells. As we are aiming for an integrated mechanism-based model for blood cancers, competition between cell types is crucial. The function of the immune system to handle dead cells constitutes an effective feedback mechanism regulating the stem cell reproduction whereas the specific T-cell response fights the cancer cells. The aggregated immune response is known to correlate with the disease state of the blood cancer. Mathematically the dynamics is described by non-linear ordinary differential equations respecting conservation laws as illustrated in figure 1.

---

[1]Named after the ancient Greek God Janus having two faces meaning that two different topologies exists.
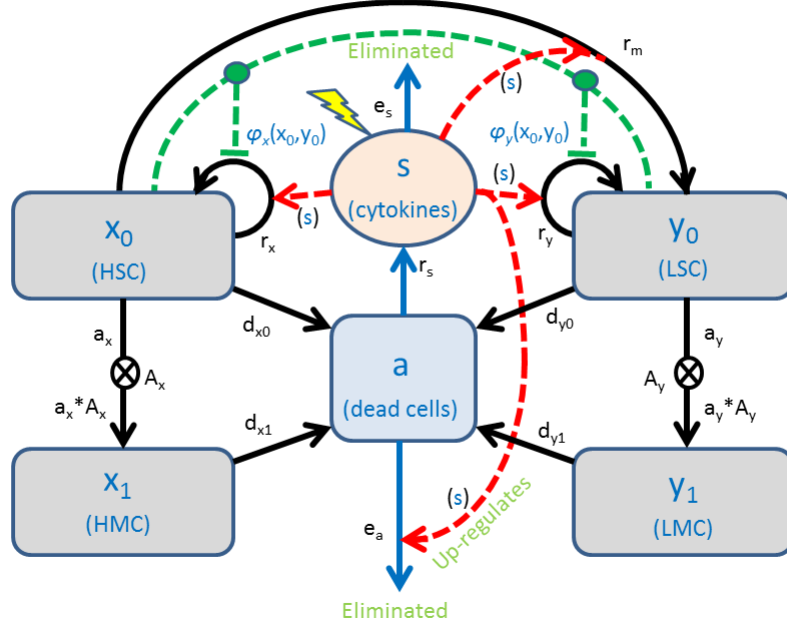
Figure 1: The conceptual model corresponding to equation (1). Light gray boxes (symbolized x_0, x_1, y_0, and y_1 for the hematopoietic stem cells (HSC), the hematopoietic mature cells (HMC), the leukemic stem cells (LSC), and the leukemic mature cells (LMC), respectively) illustrate the compartments of the basic model and the black arrows the rates of the flows between these compartments. Stem cells differentiating into progenitor cells reduce the amount of these with rates a_x and a_y and enter the corresponding mature cell-pools as these rates are multiplied by progenitor application factors (A_x and A_y, respectively, and symbolized by $\otimes$-symbols). All cells may undergo apoptosis and their death rates are indicated by black arrows labeled with a d index and the corresponding variable. A normal hematopoietic stem cell may mutate into a malignant stem cell with an effective probability r_m indicated by a black arrow. The light blue compartment (symbolized a) contains all dead cells and the light orange compartment (symbolized s) the inflammatory level, i.e. the immune response. Blue arrows from these represent related rates of flow: e_a is the second order elimination rate of debris, e_s is the elimination rate of the inflammatory activity, and r_s is the rate by which dead cells stimulate the inflammatory response. Red stipulated arrows (marked by (s)) going from the inflammatory compartment represent effects of the cytokines (or neutrophils when eliminating dead cells) modulating the rates of the basic model. The green stipulated lines represent the bone marrow niche inhibition (depending on x_0 and y_0, see text) modulating the self-renewal rates, r_x and r_y.

5

Using symbols as in figure 1 and letting dot denote the time derivative, the mathematical equations are,

$$\dot{x}_0 = (r_x \phi_x(x_0, y_0)s - d_{x_0} - a_x)x_0 - r_m s x_0 \qquad (1a)$$

$$\dot{x}_1 = a_x A_x x_0 - d_{x_1} x_1 \qquad (1b)$$

$$\dot{y}_0 = (r_y \phi_y(x_0, y_0)s - d_{y_0} - a_y)y_0 + r_m s x_0 \qquad (1c)$$

$$\dot{y}_1 = a_y A_y y_0 - d_{y_1} y_1 \qquad (1d)$$

$$\dot{a} = d_{x_0} x_0 + d_{y_0} y_0 + d_{x_1} x_1 + d_{y_1} y_1 - e_a a s \qquad (1e)$$

$$\dot{s} = r_s a - e_s s + I \qquad (1f)$$

The time dependent variables x_0, x_1, y_0, y_1, a, and s denote the amount of (healthy) hematopoietic stem cells (HSC), (healthy) hematopoietic mature cells (HMC), malignant stem cells (LSC), malignant mature cells (LMC), dead cells, and the cytokine level, an abstract quantity describing the activity level of the immune system, respectively. Whenever cells undergo apoptosis the debris has to be engulfed by phagocytic cells, e.g. neutrophils and macrophages, which are regulated by the release of a hierarchic cascade of pro- and anti-inflammatory cytokines [32, 23, 36]. Following the parsimonious principle we let the dead cells (a) up-regulate the amount of phagocytic cells (s) with rate constant r_s, while they are eliminated with a rate e_s. In addition endotoxins, smoking and other environmental factors may add to the inflammatory response; thus we add a term (characterized by the lightning symbol in Figure 1). Since MPNs develop on a time-scale of years and inflammatory immune processes are on a time-scale of hours-days ([12, 16, 14, 5]) we may assume a QSSA, implying that the ratio of the amount of phagocytic cells and the cytokines are fixed. Thus, the cytokine level is proportional to the phagocytic level and the inflammatory compartment (s) represents both.

The dynamics of the hematopoietic stem cells (x_0) are governed by the self-renewal rate r_x, the death rate d_{x_0}, and the division into progenitor cells with rate a_x. The inhibiting niche feedback in the bone marrow, represented by the function ϕ_x, controls cell division in a healthy individual and allows for competition between healthy and cancerous stem cells when both are present (see below). Furthermore, inflammation stimulates self-renewal and is assumed to be proportional with the cytokine level. This reflects the fact that an increase in hematopoietic cell death instigates the birth of extra cells. Finally, the stem cells may mutate with a mutation rate r_m, which is believed to increase with inflammation [19, 10, 39, 33, 31, 30, 70, 68, 71, 72, 2, 29].

The dynamics of the malignant stem cells (y_0) are governed similarly and we use the same symbols with an y-index instead of an x-index to denote the corresponding rates. The only difference is that mutation of hematopoietic stem cells add to the number of malignant cells and is proportional to the

number of hematopoietic stem cells. In addition, we will later allow the death rate d_{y_0} to be y_0-dependent.

If no mutations occur, stem cells divide either into two stem cells of the same type as the mother cell, into two progenitor cells, or divide into one of each. Progenitor cells differentiate further into new and gradually more and more mature progenitor cells in a number of generations (k) to ultimately divide into fully matured cells (i.e. cells which do not divide further). The progenitor cells are not explicitly considered in the model. However, a stem cell dividing into two progenitor cells, so-called symmetric division, will at the end give rise to $A = 2^k$ mature cells, which we denote as the multiplication factor. Hence, the change in hematopoietic mature cells per time becomes $a_x A_x$ times the amount of hematopoietic stem cells, where we denote A_x the multiplication factor for the hematopoietic cells, which in general is larger than 2^k. Simultaneously, hematopoietic mature cells undergo apoptosis with a constant rate d_{x_1}.

Again, the change in malignant mature cells per time is similar to that of the hematopoietic mature cells, but with index y instead of x.

The change in the amount of dead cells per time is given by the death rates times the number of cells in the afore mentioned compartments minus the clearing by the immune system. This clearing is taken to be a second order equation in the number of dead cells and the of amount of cytokines, representing the activity of the immune system, eliminating the dead cells with an elimination rate e_a.

The stimulation of the immune system is proportional to the amount of dead cells with rate r_s whereas the elimination is taken to be proportional to the amount of cytokines with rate e_s. We emphasize that the immune system is stimulated by an increased number of cancer cells by this feedback mechanism. In addition we include the possibility of an exogene stimulation of the immune system $I(t)$, where we indicate that this stimulation may change over time t. This exogene stimulation may be taken as anything provoking the immune system, e.g. infections, smoking or pollution. In many mathematical considerations we will take the inflammatory load I to be piecewise constant to allow for analytical results.

Finally, the bone marrow niche feedback functions are in general decreasing functions of the individual stem cell types. We choose

$$\phi_x = \phi_x(x_0, y_0) = \frac{1}{1 + c_{xx}x_0 + c_{xy}y_0} \tag{2a}$$

$$\phi_y = \phi_y(x_0, y_0) = \frac{1}{1 + c_{yx}x_0 + c_{yy}y_0} \, , \tag{2b}$$

where c_{ij} describes the inhibitory strength of the signaling bone marrow niche feedback from cell type j onto cell type i. It is generally assumed that $c_{yy} \leq c_{yx} < c_{xy} \leq c_{xx}$, since leukemic cells are less sensitive to inhibitive

7

niche feedback than healthy hematopoietic cells. Similar to [24] our investigations show no qualitative difference in observed model output when using various functional forms of the negative feedback.

Motivated by the biology where numbers of cells and concentrations are required to be non-negative numbers, we will use the terminology that a steady state is **admissible** if and only if all components are non-negative i.e. if and only if the steady state is in the non-negative octahedron. We denote a steady state as **appropriate** if and only if it does not require a degenerated set of parameters, i.e. a set of parameters where an equality constrain is imposed on the parameters whereas inequalities constrains are allowed. The reason is that such a set of parameters are not robust to perturbations and thus biologically unlikely to exist. However, non-appropriate steady states may still be of interest since they divide possible situations of interest like e.g. bifurcation points do.

In most considerations we take the mutation rate to be zero to ease the analytical analysis. Hence, we start our system in a steady state related to none malignant cells and introduce a single malignant stem cell initially. Thus the initial condition will be that of a (healthy) hematopoietic steady state except one malignant stem cell is added to that state.

The model stated in equations (1) and (2) is presented in [2] and will be analyzed in detail elsewhere. For later use it is sufficient to know that two admissible hematopoietic steady states (defined as one having $y_0 = 0$, but $x_0 \neq 0$) may exist depending on the level of exogenous inflammatory stimuli I,

$$E_{H\pm} = (x_{0H\pm}, x_{1H\pm}, y_{0H\pm}, y_{1H\pm}, a_{H\pm}, s_{H\pm}), \tag{3}$$

where $x_{0H\pm} = \frac{s_{H\pm} - \alpha_x}{\alpha_x c_{xx}}$, $x_{1H\pm} = \frac{a_x A_x}{d_{x_1}} x_{0H\pm}$, $y_{0H\pm} = 0$, $y_{1H\pm} = 0$, $a_{H\pm} = \frac{e_s s_{H\pm} - I}{r_s}$, and $s_{H\pm} = \frac{1}{2} \left(\zeta_{H_1} \pm \sqrt{\zeta_{H_1}^2 - 4\zeta_{H_2}} \right)$, with $\zeta_{H_1} = \frac{I}{e_s} + \frac{\zeta_{H_2}}{\alpha_x}$, $\zeta_{H_2} = \frac{\beta_x r_s}{e_a e_s c_{xx}}$, $\alpha_x = \frac{a_x + d_{x_0}}{r_x}$, and $\beta_x = a_x A_x + d_{x_0}$. These steady state coordinates will be used for turning the model into proper dimensionless form.

2.1. Model extension: Including the T-cell response

Whenever cells die, the debris have to be engulfed by phagocytic cells, e.g. neutrophils and macrophages and are regulated by a hierarchic cascade of pro- and anti-inflammatory cytokines are released. Apoptosis is mediated by the immune system and is included in the Cancitis model. The immune response may be split into two parts namely the innate immune response and the adaptive immune response [45]. The innate immune response provides an immediately but non-specific response. The innate response consists of granulocytes, dendrites, macrophages and natural killer cells. The adaptive immune response is activated by the innate immune response. Thus a delay is introduced from exposure to maximal response and this delay may be

Table 1: Default parameter values ($r_m = 0$) from [2]

Parameter	Value	Unit	Parameter	Value	Unit
r_x	$8.7 \cdot 10^{-4}$	day^{-1}	r_y	$1.3 \cdot 10^{-3}$	day^{-1}
a_x	$1.1 \cdot 10^{-5}$	day^{-1}	a_y	$1.1 \cdot 10^{-5}$	day^{-1}
A_x	$4.7 \cdot 10^{13}$	-	A_y	$4.7 \cdot 10^{13}$	-
d_{x_0}	$2 \cdot 10^{-3}$	day^{-1}	d_{y_0}	$2 \cdot 10^{-3}$	day^{-1}
d_{x_1}	129	day^{-1}	d_{y_1}	129	day^{-1}
c_{xx}	$5.6 \cdot 10^{-5}$	-	c_{yx}	$5.2 \cdot 10^{-5}$	-
c_{xy}	$5.4 \cdot 10^{-5}$	-	c_{yy}	$5.0 \cdot 10^{-5}$	-
e_s	2	day^{-1}	r_s	$3 \cdot 10^{-4}$	day^{-1}
e_a	$2 \cdot 10^9$	day^{-1}	I	7	day^{-1}

up to 7 days [45]. The adaptive immune response includes B-cells and T-cells also denoted lymphocytes. We include naive T-cells and effector T-cells, since these have an important role in inhibiting the development of cancer [43]. Effector T-cells are responsible for a direct defense, where they induce death to the malignant cells. Naive T-cells are activated by antigen presenting cells (APC). A QSSA suggests itself, since we are interested in the time-scale of years and the time-scale of the adaptive immune response is of order days.

The presence of foreign antigens in the body may be sensed by the naive T-cells (T_n). This will start a cascade of up-regulating cells and molecules in the immune system, among these effector T-cells (T_e), e.g CD8$^+$ T-cells, and NK-cells. These specifically attack and destroy the identified foreign cells (necrosis). The process from identification to attack happens on a time-scale of a week, however, the effector cells have memories to recognize the identified cells afterwards. This process is known as immune surveillance.

Inspired by Moore and Natasha [48, 49], we let the naive T-cells identify the cancer cells (we let temporarily y denote the number of such, which in our case will be y_0 or y_1). These T-cells are transformed into effector cells proportional to the product of the number of naive T-cells and cancer cells with rate, k_n. Naive T-cells may produce α_n effector cells per transforming naive T-cell. A linear elimination of naive T-cells appear simutaneously with rate ηk_n. The naive T-cells are produced at a constant rate p_n, whereas effector cells are eliminated proportional to T_e with rate γ_e. Thus,

$$\dot{T}_n = p_n - k_n T_n(y + \eta) \tag{4}$$

and

$$\dot{T}_e = \alpha_n k_n T_n y - \gamma_e T_e. \tag{5}$$

The pool of effector cells (T_e) eliminate the cancer cells as a second order reaction with rate γ_y. Letting 'growth' denote the aforementioned dynamics

of cancer cells without explicitly including the T-cells, i.e. the right hand side of equation (1c) or (1d), the governing equation of malignant cells become

$$\dot{y} = \text{growth} - \gamma_y T_e y. \tag{6}$$

The fast T-cell response compared to the slow timescale of MPNs development justify a QSSA, thus

$$T_e \approx \frac{\alpha_n p_n}{\gamma_e} \frac{y}{y + \eta} \tag{7}$$

and

$$\dot{y} = \text{growth} - \frac{\gamma_y \alpha_n p_n}{\gamma_e} \frac{y^2}{\eta + y} \approx \text{growth} - \tilde{d}_y y^2, \tag{8}$$

with $\tilde{d}_y = \frac{\gamma_y \alpha_n p_n}{\gamma_e \eta}$ and where the approximation holds if $y \ll \eta$. Hence, using the approximation in equation (8) the death rate d_y in the 'growth' part may be substituted by

$$d_y \rightarrow \hat{d}_y + \tilde{d}_y \frac{\eta\, y}{\eta + y} \approx \hat{d}_y + \tilde{d}_y \cdot y \tag{9}$$

for $y \ll \eta$ where $\hat{d}_y = d_y$. Thus, the constant mortality rate is changed by adding a death rate which is linear in y. In fact, this may be considered as a general approximation of a possible y-dependent death rate by its first order Taylor expansion. We emphasize that this expression is desirable, since it is still simple, but includes an important effect for non-vanishing values of y. A reasonable choice is to take $\hat{d}_y = d_{y0}$ and $\tilde{d}_y \sim 10^{-6}$ day^{-1} as default values. These estimates are based on requiring the two elimination terms to be of the same order and equal to that for normal hematopoietic stem cells, which is approximately 0.002 cell per day [20, 2].

Hence, the leukemic model in equation (1) still holds with d_{y0} substituted by $\hat{d}_{y0} + \tilde{d}_{y0} \cdot y_0$ where we assume that the most important effect is on the stem cell compartment, which drives the cancer development. The previous analytical results obtained are corrupted by the extension allowing the death rate to be y_0 dependent. We therefore seek a suitable model reduction (obtained in equation (10)) allowing a more thorough analysis.

2.2. Model validation

In the stable hematopoietic steady state the numbers of stem cells and mature cells are taken to be approximately 10^4 and $4 \cdot 10^{10}$, respectively, which are compromises between reported values [26, 27, 25, 62, 63, 20]. In the final stage of full blown cancer, the number of hematopoietic cells is vanishing and the cancer cells will approach a stable steady state with a higher amount of cells than in the healthy steady state. The absolute values are more uncertain but we have aimed for 10^5 cancer stem cells and 10^{13}

mature cancer cells as reported in [20]. In clinical practice JAK2V617 allele burden and the total cell count in the blood are usually measured. Whereas the total cell count is $x_1 + y_1$, the JAK2V617 allele burden is taken as $\frac{y_1}{x_1+y_1}$. The JAK2V617 allele burden has been reported to have median values of 7% (95% CI 2-15% and range 1-39%), 33% (95% CI 20-40% and range 1-92%), and 67% (95% CI 52-95% and range 37-99%) in ET, PV and PMF patients, respectively [44]. The model is calibrated to resample this dynamic in the JAK2V617F allele burden, which gives predictions, t_{ET}, t_{PV}, and t_{PMF} for when ET, PV and PMF appear, respectively. For illustrations of cell counts and allele burden see Fig. 2 Cytokines as IL-1β, IL-1RA, IL-2R, IL-6, IL-8, IL-10, and IL-12 are considered to be specific indicators of the inflammatory level during MPN, whereas C-reactive protein (CRP) is a general inflammation biomarker. All these have been shown to correlate with MPN states ET, PV and PMF. [66, 67] Thus we assume linear correlations between each of these and the inflammatory level s. In addition LDH values, which express the total rate of dying cells per time $(D = d_{x_0} x_0 + d_{x_1} x_1 + d_{y_0} y_0 + d_{y_1} y_1)$ were demonstrated to be correlated to the MPN states ET, PV and PMF [44]. The model outputs are compared to the data in Fig. 3. using the estimated instances t_{ET}, t_{PV}, and t_{PMF} for ET, PV and PMF, respectively. The model predictions are in a remarkable accordance with the data.

3. The reduced Cancitis model

The extended model is brought into dimensionless form by scaling the variables of the model. A time scale separation argument is used to obtain a reduced model, corresponding to setting the time derivative of x_1, y_1, a, and s to zero. The four dependent variables may then be solved in terms of x_0 and y_0. As this approach is well known and straightforward, the derivation is shown in appendix Appendix A. Analyzing the resulting equations (10) in terms of the scaled hematopoeitic stem cells, X_0, and the scaled cancerous stem cells, Y_0, is the focus of the rest of the paper.

$$X_0{}' = \left(\frac{J + \sqrt{J^2 + 2B_x X_0 + 2B_y Y_0}}{1 + X_0 + C_y Y_0} - 1 \right) X_0 \tag{10a}$$

$$Y_0{}' = \left(R \frac{J + \sqrt{J^2 + 2B_x X_0 + 2B_y Y_0}}{1 + C_x X_0 + Y_0} - D_0 - D_1 Y_0 \right) Y_0 \tag{10b}$$

where $J = \frac{I}{2e_s} \frac{r_x}{d_{x_0}+a_x}$, $R = \frac{r_y}{r_x}$, $D_0 = \frac{\hat{d}_{y_0}+a_y}{d_{x_0}+a_x}$, $D_1 = \frac{\tilde{d}_{y_0}}{c_{yy}} \frac{1}{d_{x_0}+a_x}$, $C_x = \frac{c_{yx}}{c_{xx}}$, $C_y = \frac{c_{xy}}{c_{yy}}$, $2B_x = b_{x_0} + b_{x_1} \approx b_{x_1} = \frac{a_x A_x}{c_{xx}} \frac{r_s}{e_s e_a} \frac{r_x}{d_{x_0}+a_x} \sim 10^{-1}$, and $2B_y = b_{y_0} + b_{y_1} \approx b_{y_1} = \frac{a_y A_y}{c_{yy}} \frac{r_s}{e_s e_a} \frac{r_x}{d_{x_0}+a_x} \sim 10^{-1}$. Notice, the ratio between B_x and
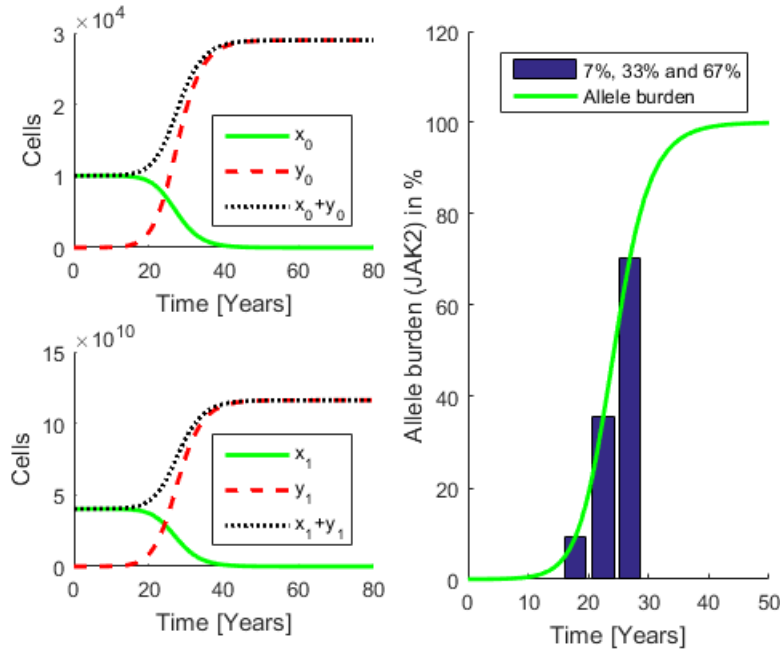
Figure 2: Left: Typical development in stem cells (top left) and mature cells (bottom left). Healthy hematopoietic cells (full green curves) dominate in the early phase where the malignant cells (stipulated red curves) are few in number. The total number of cells is also shown (dotted black curves). When a stem cell mutates and escapes repairing mechanisms, it approximately starts a slowly increasing exponential growth (at $t = 0$). At a certain stage the malignant cells become dominant and the healthy hematopoietic cells begin to show a visible decline. Finally, the competition between the cell types results in a takeover by the malignant cells, leading to an approximately exponential decline in the amount of normal hematopoietic cells and ultimately their extinction. The development is closely followed by the mature cells. Right: The corresponding allele burden (7%, 33% and 67% corresponding to ET, PV and PMF, respectively, shown as blue columns) defined as the ratio of MPN mature cells to the total number of mature cells. The full green curve illustrates the continuous model prediction. Default parameter values from table 1 and 2 have been used.
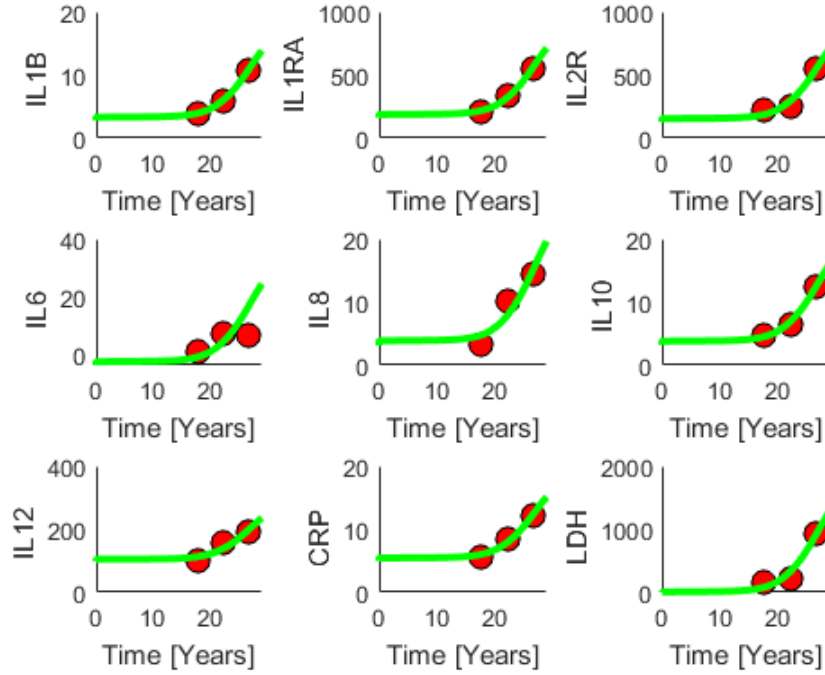
12

Figure 3: Model validation. Cytokines from upper left to lower right; IL-1β, IL-1RA, IL-2R, IL-6, IL-8, IL-10, IL-12 as well as the plasma concentration of C-reactive protein (CRP) are approximatively linearly correlated with the inflammatory level s, whereas lactic dehydrogenase (LDH) is linearly correlated with and compared to the total amount of dying cells per time $D = d_{x_0}x_0 + d_{x_1}x_1 + d_{y_0}y_0 + d_{y_1}y_1$. On each subplot data are shown (red dots encircled by black) at predicted times for ET, PV and PMF (left to right) estimated from the allele burden in Fig.2. On each subplot model predictions are shown (full green curve). Default parameter values from table 1 and 2 have been used.

B_y is the ration between the rate by which the corresponding mature cells are produced normalized by their self-inhibitory factor (carrying capacity).

The default dimensionless parameter values are listed in table 2. Note, the reduced model involves 8 parameters where D_1 describe the strength of the Y_0 dependent elimination term in dimensionless form. The numerator in equation (10) corresponds to the scaled cytokine level and the denominators express the stem cell niche interactions allowing for different competitive advantages of hematopoietic and cancerous cells. The death rate of hematopoietic stem cells has been normalized to 1, whereas a different rate is allowed for cancer stem cells (D_0) as well as an extra degradation term ($D_1 Y_0$) corresponding to the T-cell response. We emphasize the local existence and uniqueness of solutions in the non-negative octahedron. Subsequently we will focus on the impact of the dimensionless inflammatory stimuli J.

Table 2: Default dimensionless parameter values ($r_m = 0$)

Parameter	Value	Parameter	Value
R	1.49	J (baseline)	0.76
D_0	1.00	D_1	0.10
C_x	0.93	C_y	1.08
B_x	0.06	B_y	0.07

Figure 4 illustrates that the reduced cancitis model agrees excellently with the full model for various values of D_1. As seen, an increase in the Y_0-dependent death rate, corresponding to how aggressively the effector cells eliminate the malignant stem cells, conjures a bearable co-existing state. Higher values of D_1 yields a lower burden of malignant cells. This is in accordance with the concept of immune surveillance (as illustrated in figure 4 for $D_1 = 5$), [55]. If resistance appears, i.e. the malignant cells become immune to the effector cells, it agrees with the concept of immunoediting [55]; In the first phase malignant cells are killed (not pictured in figure 4), in the second phase a pseudo-equilibrium between immune and malignant cells appears (as for $D_1 = 5$ in figure 4), and finally the third phase - the escape phase - develops, where the co-existing pseudo-steady state disappears due to an absence of a sufficient immune response. In the escape phase the disease ultimately gives symptoms and it may become clinically detected (as for $D_1 = 0.1$ in figure 4). The absence of a sufficient immune response is believed to be caused by a down-regulation or loss of an expression of malignant antigens, an upregulated resistance of malignant cells, an increased expression of pro-survival genes, or the development of an immunosuppressive malignant cell microenvironment. [55]
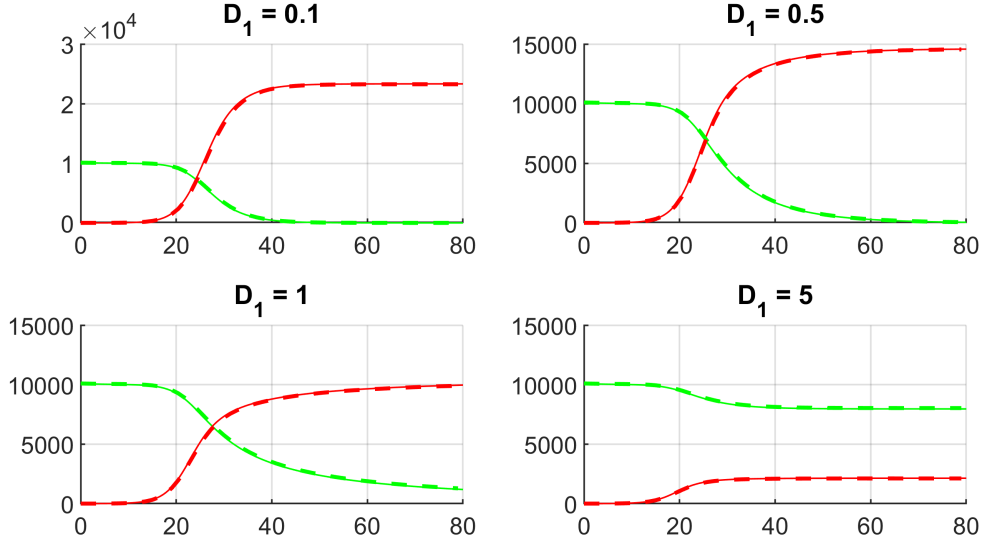
14

Figure 4: Comparison of the reduced model (stipulated curves) and the full model (full curves) for dimensionless values $D_1 = 0.1, 0.5, 1, 5$. Green curves show hematopoietic stem cell counts and red curves show malignant stem cell counts versus time in years. All quantities are in dimensional variables.

4. Analysis and results

We study the effect of the dimensionless inflammatory load J on the possible steady states and their stability for the reduced cancitis model in equation (10). Thus, we start by investigating the existence of steady states. By definition

- A trivial steady state is defined as having $X_0 = Y_0 = 0$.

- A (purely) hematopoietic steady state is defined as having $Y_0 = 0$, but $X_0 > 0$.

- A (purely) leukemic steady state is defined as having $X_0 = 0$, but $Y_0 > 0$.

- A co-existing steady state is defined as having $X_0 > 0$ and $Y_0 > 0$.

Note, non-negativity of X_0 and Y_0 implies non-negativity of the derived variables X_1, Y_1, A, and S_+ given by equation (A.9). Straight forward, but tedious computations (see Appendix B) give analytical results for the steady states, which are summarized as,

- An admissible **trivial steady state** always exists,

$$F_0 = (0, 0). \tag{11}$$

15

- Admissible **hematopoietic steady states**, $F_H = (X_{0H}, 0)$ are solutions to

$$\frac{J + \sqrt{J^2 + 2B_x X_{0H}}}{1 + X_{0H}} - 1 = 0, \qquad (12)$$

with $X_{0H} > 0$. For certain combinations of parameter values two solutions may exist,

$$X_{0H\pm} = J + B_x - 1 \pm \sqrt{(J + B_x - 1)^2 + 2J - 1}. \qquad (13)$$

For $F_{H\pm}$ to be admissible all components have to be real and non-negative and X_0 have to be positive. This gives rise to some restrictions given as inequalities in the level of exogenous inflammatory stimuli.

  – For $B_x < \frac{1}{2}$ no admissible hematopoitic steady state exists for $J \leq \frac{1}{2}$. A bifurcation happens at $J = \frac{1}{2}$ such that for $J > \frac{1}{2}$ a unique, admissible hematopoetic steady state, X_{0H+}, exists with $X_{0H+}(J) \to 0$ for $J \to \frac{1}{2}$ and $X_{0H+}(J)$ being an increasing function.

Note, both the existence and the value of X_{0H+} only depends on the two parameters J and B_x. Remarkably, increasing the dimensionless rate $B_x \approx \frac{r_s}{c_{xx} e_s e_a}$, by which the normal cells stimulate the dead cell pool, leads to an increase in the amount of normal cells X_{0H+} at the hematopoietic steady state value.

- Admissible **purely leukemic steady states**, $F_L = (0, Y_{0L})$, are the solutions of

$$R\frac{J + \sqrt{J^2 + 2B_y Y_{0L}}}{1 + Y_{0L}} - D_0 - D_1 Y_0 = 0, \qquad (14)$$

with $Y_{0L} > 0$.

  – For $J > \frac{1}{2}\frac{D_0}{R}$ a unique, admissible leukemic steady state exists. Then $Y_{0L}(J)$ is increasing in J.

  – For $B_y < \frac{1}{2}\frac{D_0}{R}\left(\frac{D_0}{R} + \frac{D_1}{R}\right)$, and $J < \frac{1}{2}\frac{D_0}{R}$ no leukemic steady states exist.

  – For default parameter values, $B_y < \frac{1}{2}\frac{D_0}{R}\left(\frac{D_0}{R} + \frac{D_1}{R}\right)$ and increasing inflammatory stimuli passing the critical value $J_{crit} = \frac{1}{2}\frac{D_0}{R}$, a leukemic steady state is created. This happens as $Y_0(J)$ increases from 0 with increasing J.

Note, both the existence and the value of a leukemic steady state only depends on the four parameters J, $\frac{D_0}{R}$, $\frac{D_1}{R}$, and B_y.

- **Co-existing steady states**, $F_C = (X_{0C}, Y_{0C})$, may exist, being the solutions of

$$J + \sqrt{J^2 + 2B_x X_{0C} + 2B_y Y_{0C}} = 1 + X_{0C} + C_y Y_{0C} \qquad (15)$$

and

$$J + \sqrt{J^2 + 2B_x X_{0C} + 2B_y Y_{0C}} = (1 + C_x X_{0C} + Y_{0C})\left(\frac{D_0}{R} + \frac{D_1}{R} Y_{0C}\right), \qquad (16)$$

where $X_{0C} > 0$ and $Y_{0C} > 0$. X_{0C} can be computed directly, if Y_{0C} is known,

$$X_{0C} = \frac{(1 + Y_{0C})\left(\frac{D_0}{R} + \frac{D_1}{R} Y_{0C}\right) - C_y Y_{0C}}{1 - C_x \left(\frac{D_0}{R} + \frac{D_1}{R} Y_{0C}\right)}. \qquad (17)$$

Candidates for Y_{0C} are solutions to a fourth order polynomial with intricate expressions for the coefficients not easily investigated analytically. The co-existing steady state is not created by a bifurcation through $(0, 0)$ as no solution to (15) and (16) exists for (X_{0C}, Y_{0C}) approaching this point. Instead the co-existing steady state bifurcates from either the hematopoietic or the leukemic steady state, depending on the stability properties of these.

4.1. Stability considerations

In this section we examine the stability properties of the various admissible steady states of the reduced model. The stability of the steady states are equivalent to the stability of the linearized equations near the steady state, if the steady state is hyperbolic, i.e. if no eigenvalue of the matrix of the linearized system has real part equal to zero. The Jacobian, $\mathcal{J}$, of equation (10) is computed analytically at most of the steady states, see below. Thus, for these steady states, the eigenvalues of the linearized system are easily obtained analytically and otherwise numerically. If all eigenvalues have negative real part, the steady state is stable and attracts neighbouring solutions, while if at least one eigenvalue has positive real part, the steady state is unstable. For the trivial steady state, the leukemic steady state and the hematopoietic steady state, $\mathcal{J}$ is calculated analytically and becomes triangular, thus the eigenvalues can be directly read off from the diagonal.

In this section we focus on cases that may be investigated analytically and in accordance with the default parameters we therefore assume,

$$B_x < \frac{1}{2}, \quad \text{and} \quad B_y < \frac{1}{2}\frac{D_0}{R}\left(\frac{D_0}{R} + \frac{D_1}{R}\right), \qquad (18)$$

which were also used in the previous section for clear statements on existence of a hematopoietic and a leukemic steady state, respectively. In the following we investigate the stability of the steady states.

First, consider the **trivial steady state**. At F_0 the Jacobian for the trivial steady states becomes,

$$\mathcal{J}_0 = 2 \begin{bmatrix} J - \frac{1}{2} & 0 \\ 0 & R\left(J - \frac{D_0}{2R}\right) \end{bmatrix}.$$ (19a)

with eigenvalues $\lambda_1 = J - \frac{1}{2}$ and $\lambda_2 = J - \frac{D_0}{2R}$. Evidently the two eigenvalues are negative if and only if $J < \min\{\frac{1}{2}, \frac{D_0}{2R}\}$. Compared to the previous section this implies that the trivial steady state is stable only if there are no leukemic or hematopoietic steady states.

Secondly, consider the **hematopoietic steady state** and the corresponding Jacobian, $\mathcal{J}_H$, with the form

$$\mathcal{J}_H = \begin{bmatrix} \lambda_{H1} & \mathcal{J}_H(1,2) \\ 0 & \lambda_{H2} \end{bmatrix},$$ (20a)

where

$$\mathcal{J}_H(1,2) = X_{0H+} \frac{B_y\left(1 + X_{0H+}\right) - C_y\sqrt{J^2 + 2B_xX_{0H+}}\left(J + \sqrt{J^2 + 2B_xX_{0H+}}\right)}{\sqrt{J^2 + 2B_xX_{0H+}}\left(1 + X_{0H+}\right)^2}.$$ (21)

The Jacobian is an upper triangular matrix with vanishing entry (2,1), i.e. $\mathcal{J}_H(2,1) = 0$, and the eigenvalues are given by the diagonal entries. The first eigenvalue $\lambda_{H1} = \mathcal{J}_H(1,1)$ has corresponding eigenvector pointing along the X_0 - axis. The expression of λ_{H1} can be formulated

$$\lambda_{H1} = \frac{X_{0H+}}{\left(1 + X_{0H+}\right)\sqrt{J^2 + 2B_xX_{0H+}}}\left(-\sqrt{(J + B_x - 1)^2 + 2J - 1}\right).$$ (22)

Whenever the hematopoietic steady state is admissible, $X_{0H+} > 0$ corresponding to $J > \frac{1}{2}$, the eigenvalue is negative, $\lambda_{H1} < 0$. Thus, if the dynamics is restricted to the X_0-axis then X_{0H+} is stable. This is a desirable property of the model as it illustrates that homeostasis is maintained prior to a mutation providing a malignant stem cell.

The other eigenvalue is

$$\lambda_{H2} = R\left(\frac{1 + X_{0H+}}{1 + C_xX_{0H+}} - \frac{D_0}{R}\right).$$ (23)

As X_{0H+} does neither depend on C_x nor $\frac{D_0}{R}$ a direct inspection of equation (23) yields that increasing C_x or $\frac{D_0}{R}$ has a stabilizing effect.

Since X_{0H+} increases from 0, as J increases from $\frac{1}{2}$, the hematopoietic steady state bifurcating from the trivial steady state is stable if $\frac{D_0}{R} > 1$ and unstable if $\frac{D_0}{R} < 1$ for J in a neighborhood of and larger than $\frac{1}{2}$. Note, if

18

$C_x \geq 1$ then $\frac{1+X_{0H+}}{1+C_x X_{0H+}} \leq 1$. Hence, if $\frac{D_0}{R} > 1$ and $C_x \geq 1$, which corresponds to the malignant cells are inhibited more than the hematopoietic cells by the niche feedback, then the hematopoietic steady state is stable for arbitrarily large X_{0H+}. For $C_x < \frac{R}{D_0} < 1$, the stable hematopoietic steady state will turn unstable for sufficiently large J, since λ_{H2} approaches $C_x^{-1} - \frac{D_0}{R} > 0$ as X_{0H+} increases unboundedly with J. Rewriting $\lambda_{H2} = 0$ by use of equation (12) one arrives at the criterion

$$R\frac{J + \sqrt{J^2 + 2B_x X_0 + 2B_y Y_0}}{1 + C_x X_0 + Y_0} - D_0 - D_1 Y_0 = 0 \tag{24}$$

at $Y_0 = 0$ corresponding to the coexisting steady state being extended to the Y_0 axis (see expression (16)). This means that the hematopoietic steady state changes stability when it crosses a branch of the co-existing steady state on the X_0-axis and is unstable for large values of X_{0H+} corresponding to large values of J. The criterion $\lambda_{H2} = 0$ is easily solved for a critical X_{0H+}-value, X_c,

$$X_c = \frac{\frac{D_0}{R} - 1}{1 - \frac{D_0}{R}C_x}. \tag{25}$$

As X_{0H+} is an invertible function of J, equation (25) may be expressed as a threshold value of J,

$$J_c = \frac{X_c^2 + 2(1 - B_x)X_c + 1}{2(1 + X_c)}. \tag{26}$$

Thirdly, consider the **purely leukemic steady state**, and the corresponding Jacobian, $\mathcal{J}_L$,

$$\mathcal{J}_L = \begin{bmatrix} \lambda_{L1} & 0 \\ \mathcal{J}_L(2,1) & \lambda_{L2} \end{bmatrix}, \tag{27a}$$

with

$$\mathcal{J}_L(2,1) = RY_{0L}\frac{B_x\left(1 + Y_{0L}\right) - C_x\sqrt{J^2 + 2B_y Y_{0L}}\left(J + \sqrt{J^2 + 2B_y Y_{0L}}\right)}{\sqrt{J^2 + 2B_y Y_{0L}}\left(1 + Y_{0L}\right)^2}. \tag{28}$$

The Jacobian is a lower triangular matrix. Since entry (1,2) vanish, $\mathcal{J}_L(1,2) = 0$, the Y_0-axis is the eigenvector direction for the eigenvalue $\lambda_2 = \mathcal{J}_L(2,2)$ evaluated at the leukemic steady state. Using the restrictions on B_y from inequality (18) we get

$$\lambda_{L2} = Y_{0L}\left(\frac{RB_y}{\sqrt{J^2 + 2B_y Y_{0L}}\left(1 + Y_{0L}\right)} - R\frac{J + \sqrt{J^2 + 2B_y Y_{0L}}}{\left(1 + Y_{0L}\right)^2} - D_1\right)$$

$$\leq -D_1 Y_{0L}^2, \tag{29}$$

19

so the leukemic steady state is stable along the direction of the Y_0-axis. The other eigenvalue is

$$\lambda_{L1} = \left(\frac{D_0}{R} + \frac{D_1}{R} Y_{0L} \right) \frac{1 + Y_{0L}}{1 + C_y Y_{0L}} - 1 . \tag{30}$$

As Y_{0L} increases from 0 as J increases from $\frac{1}{2} \frac{D_0}{R}$, then $\lambda_{L1} < 0$ if $\frac{D_0}{R} < 1$ and $\lambda_{L1} > 0$ if $\frac{D_0}{R} > 1$, for J values near $\frac{1}{2} \frac{D_0}{R}$. Increasing C_y has a stabilizing effect by decreasing λ_{L1}. Contrary to the hematopoietic case, an initial negative λ_{L1} will inevitably become positive for increasing J, after which Y_{0L} increases unboundedly causing the first term in equation (30) to become larger than one. The analytical results for existence and stability of the trivial, hematopoietic and leukemic steady states are summarised in figure 5.

Lastly, consider the **co-existing steady state**. The admissible co-existing steady states are calculated numerically as a function of J and so is the Jacobian and its eigenvalues using the parameter values in table 2 for the remaining parameters when nothing else is specified. The results are summarized in figure 8 and admissible co-existing steady states are stable for $J > 3.636$ approximately. The model implies that the ratio between R and the cell death rate D_0 is important. If the ratio between D_0 and R is less than one, the leukemic steady state is stable when created and occurs before the unstable hematopoietic steady state occurs for J increasing until the co-existing steady state may take over the stability and bifurcate from the leukemic steady state. This is not to say that an increase in the inflammatory load cures the *in silico* patient or that it reduces the impact of the disease. Instead the co-existing steady state level of the malignant cells saturates approximately at the level as the level of malignant cells at the full leukemic steady state at the bifurcation point. Thus the tumor burden is not decreased, but is only prevented from increasing significantly. See Fig 6 and 8. This model based hypothesis may seem a little counter-intuitive and deserves clinical testing. Conversely if, the ratio between D_0 and R is larger than one, the hematopoietic steady state is born stable and occurs before the unstable leukemic steady state occurs for J increasing until the co-existing steady state may take over the stability of - and bifurcate from - the hematopoietic steady state, see figure 7. Hence we emphasize that the dynamics of the system is rather different depending on whether the ratio between D_0 and R is less than or greater than one. Thus increasing the ratio D_0 to R or increasing the ratio of D_1 to R, as illustrated in Fig. 7, represent very appealing candidates for treatment. Equation (B.11) is equivalent to equation (B.18) with $X_0 = 0$, thus the leukemic steady state and the co-existing steady state equals for $X_0 = 0$. By the implicit function theorem it follows that for $Y_0 \geq Y_{0L}$ the derivative of $X_0 = X_0(Y_0)$ with respect to Y_0 is positive corresponding to an increasing steady state trajectory in J.
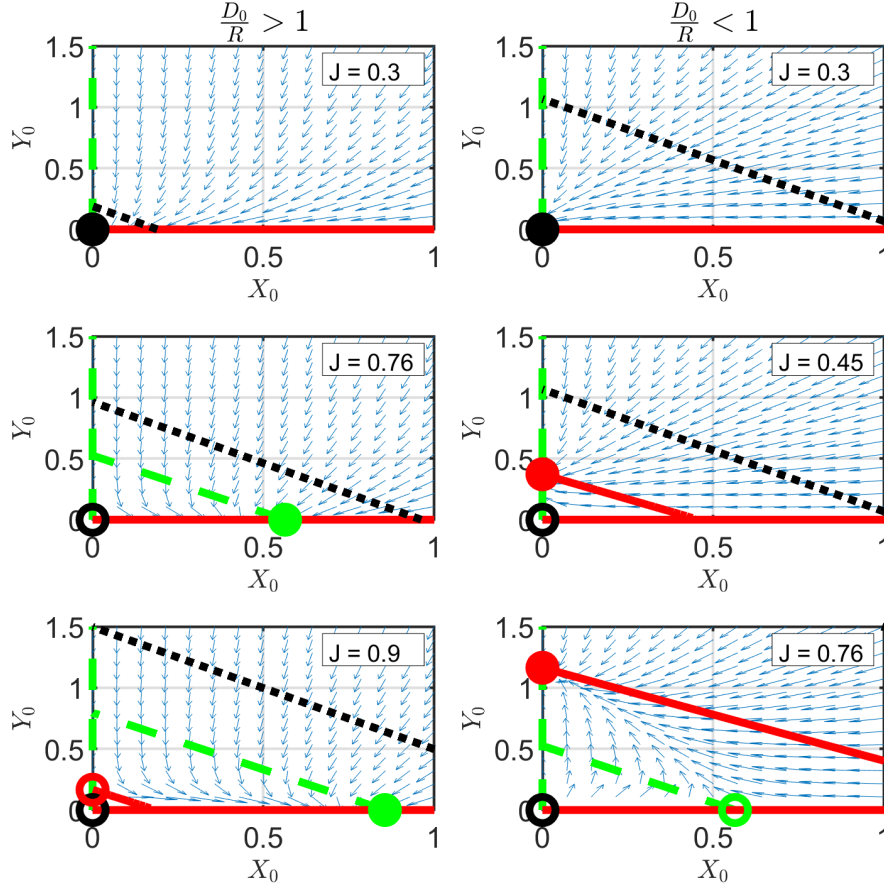
Figure 5: Phase plane diagram for the hematopoietic cells (X_0) and the leukemic cells (Y_0). The cases corresponding to analytical results of the trivial, hematopoietic and leukemic steady states and their stability are shown. J increases from top row to bottom row illustrating the sequence of bifurcations for increasing J in the two cases $\frac{D_0}{R} > 1$ and $\frac{D_0}{R} < 1$. Full circles are stable steady states, open circles are unstable steady states. The black dotted line is the boundary of the analytical trapping region, the red curve is nullcline of $\dot{Y}_0$, and the green stipulated curve is the nullcline of $\dot{X}_0$. In the left column the hematopoietic steady state is stable independently of the presence of a leukemic steady state whereas in the right column, the leukemic steady state is stable. We emphasize that the trapping region generally depends on D_0 and J as well as R, B_x, B_y, C_x, and C_y. On some subplots the dotted black line lies outside the visible rage.

The possible topologies are summarized in figures 6 and 7. The corresponding bifurcation diagram are depicted in figure 8. Continuous animations for varying J for different fixed values of D_0 and D_1 may be found at http://dirac.ruc.dk/cancitis/ together with an animated bifurcation diagram (see subsection 4.3 for further discussions). We refer to the topology of the dynamical system as Janus topology, since it has two faces, i.e. two different topologies for different set of parameters.

4.2. Existence af an attracting trapping region for the reduced cancitis model

A trapping region is a compact set with the property that orbits starting in the trapping region cannot escape the region. An attracting trapping region is a trapping region which is attracting, i.e. orbits starting outside the trapping region will enter the trapping region (in finite time). An attracting trapping region is a suitable feature for a biological system, since it guaranties some basic well-behavior of the system such as boundedness of solutions and global existence in time [56].

An attracting trapping region exists in the non-negative octahedron for the reduced cancitis model in equation (10) (will be shown below). As a consequence the steady states lies in this trapping region.

For some parameter values, $X_0' < 0$ and $Y_0' < 0$ for any X_0 and Y_0. The idea is to show that $X_0' < 0$ and $Y_0' < 0$, for large $X_0 + Y_0$ for all parameter values.

Let

$$K = \max\{J, \sqrt{2B_x}, \sqrt{2B_y}\} \quad \text{and} \quad L = \min\{1, C_x, C_y\}. \tag{31}$$

Thus, $J^2, 2B_x, 2B_y < K^2$ and $1, C_x, C_y > L$, which implies

$$\frac{J + \sqrt{J^2 + 2B_x X_0 + 2B_y Y_0}}{1 + X_0 + C_y Y_0} - 1 < \frac{K}{L} \frac{1 + \sqrt{1 + X_0 + Y_0}}{1 + X_0 + Y_0} - 1, \tag{32}$$

and

$$R \frac{J + \sqrt{J^2 + 2B_x X_0 + 2B_y Y_0}}{1 + C_x X_0 + Y_0} - D_0 - D_1 Y_0$$
$$< R \frac{K}{L} \frac{1 + \sqrt{1 + X_0 + Y_0}}{1 + X_0 + Y_0} - D_0 \tag{33}$$

Consider therefore (for $\alpha > 0$)

$$\alpha \frac{1 + \sqrt{1 + X_0 + Y_0}}{1 + X_0 + Y_0} - 1, \tag{34}$$

and introduce

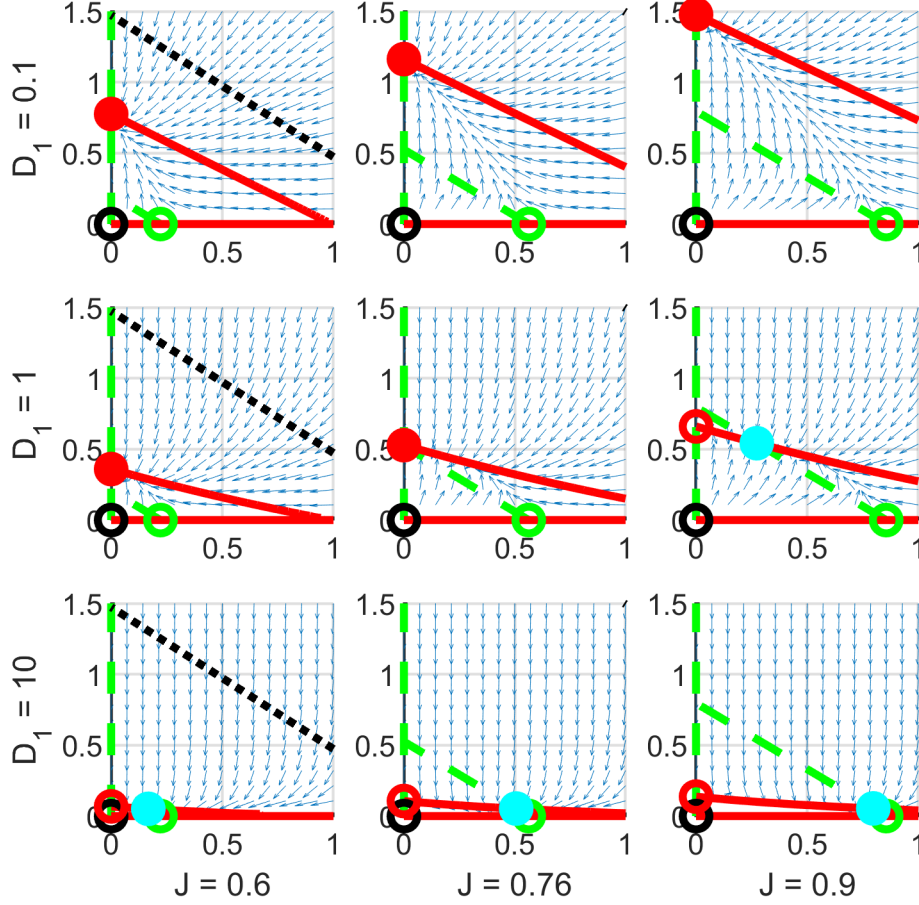$$z = \sqrt{1 + X_0 + Y_0}. \tag{35}$$

22

Figure 6: Illustration of the dynamics in a (X_0, Y_0)-phase plane. Each row corresponds to $D_1 = 0.1, 1, 10$, respectively, whereas each column corresponds to $J = 0.60, 0.76, 0.90$, respectively. Red curves are Y_0 null clines (includes the X_0-axis) and blue stipulated curves are X_0 null clines (includes the Y_0-axis). Open circles represent unstable steady states whereas full circles represent stable steady states. The black circle is the trivial steady state, the green circle the hematopoietic steady state, the red the purely leukemic steady state, and cyan the co-existing steady state. The attracting trapping region is indicated on each palette by the coordinate axis and a black dotted line, which increases with J but has slope -1 (the black dotted line may fall outside the visible range on some subplots). The flows are indicated by the normalized slope field with arrows.
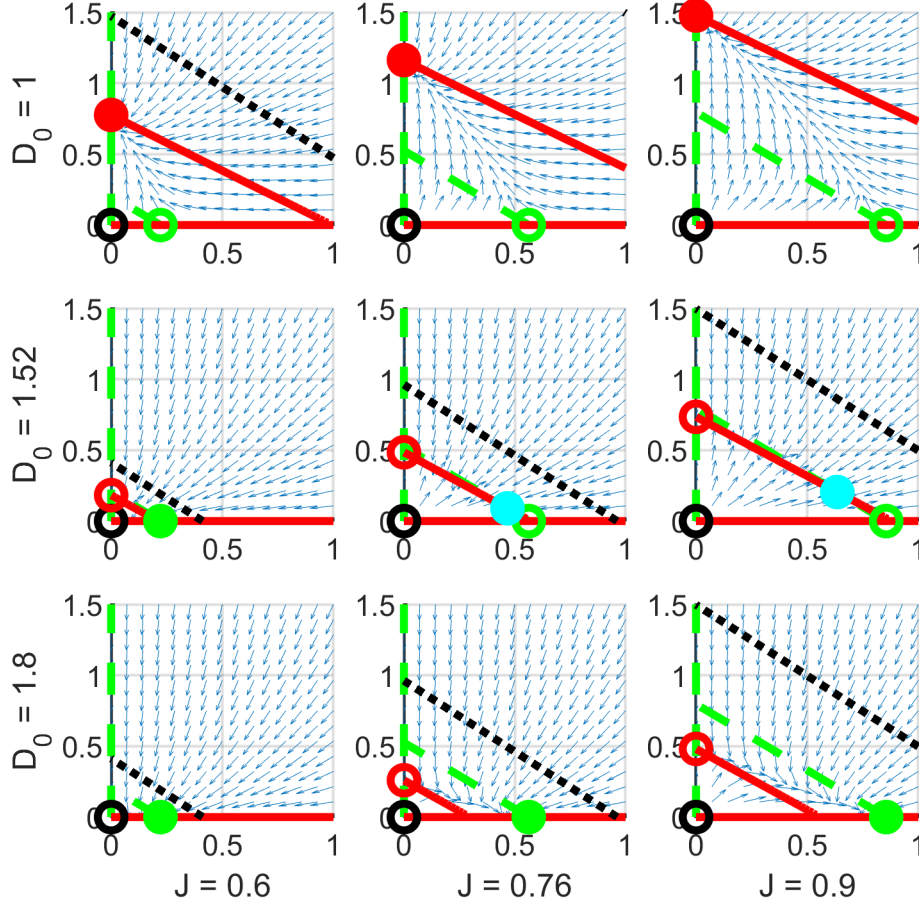
Figure 7: Illustration of the dynamics in the (X_0, Y_0) phase plane. Each row corresponds to $D_0 = 1, 1.52, 1.8$, respectively, whereas each column corresponds to $J = 0.60, 0.76, 0.90$, respectively. R is set to its default value 1.49. Red curves are Y_0 nullclines (and include the X_0-axis) and green stipulated curves are X_0 nullclines (and include the Y_0-axis). Open circles represent unstable steady states whereas full circles represent stable steady states. The black circle is the trivial steady state, the green circle the hematopoietic steady state, the red circle the purely leukemic steady state, and the cyan circle the co-existing steady state. The attracting trapping region is indicated on each palette (surrounded by the coordinate axis and a black dotted line, which may fall outside the visible rage). The trapping region decreases with D_0 and increases with J, but has slope -1. The flows are indicated by the normalized slope field with arrows.
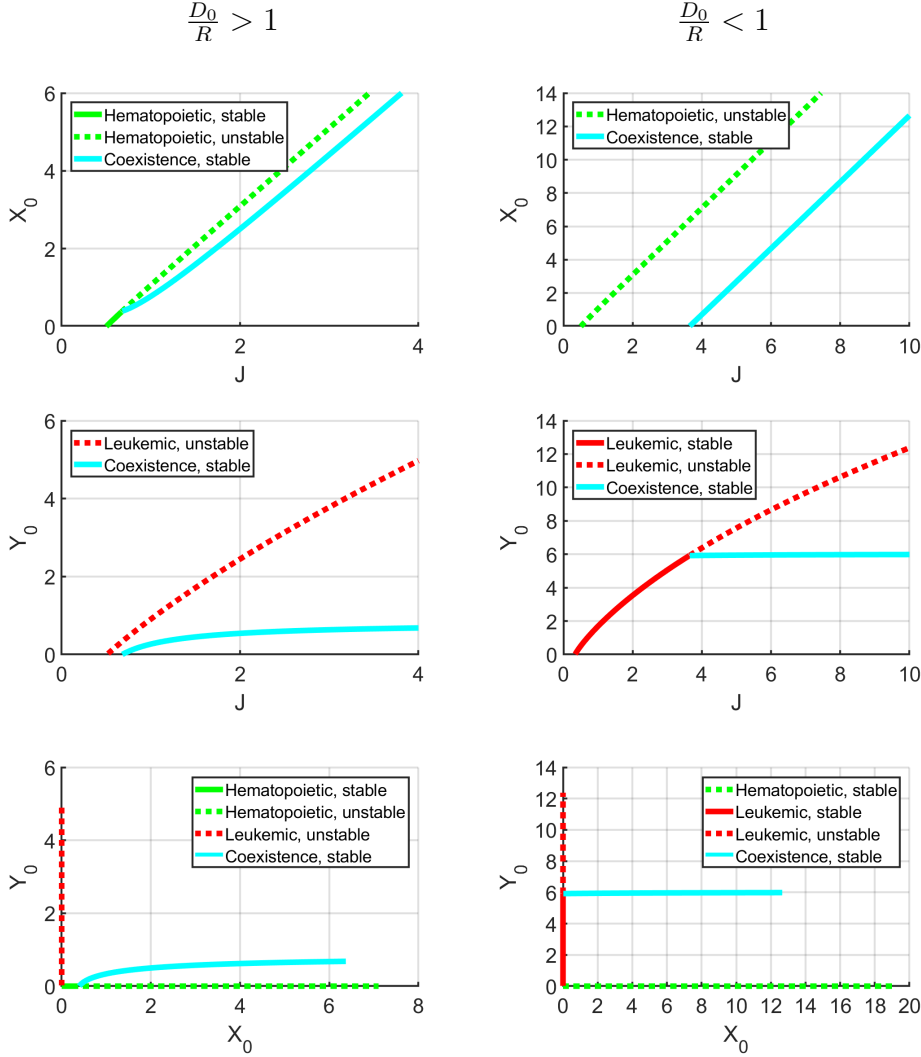
Figure 8: Left column shows the bifurcation diagrams for the case $\frac{D_0}{R} > 1$ and the right column shows the corresponding for $\frac{D_0}{R} < 1$ (the default case). The bifurcation diagrams showing the appearance and stability of the admissible steady states depending on the bifurcation parameter J. The top panel shows X_0, the middle panel shows Y_0, and the lower panel shows the J-trajectory of the admissible steady states in a (X_0, Y_0) phase plane having the range on the axis as in the other figures above. Green curves are the hematopoietic steady states, red curves are the purely leukemic steady states, and cyan curves are the co-existing steady states. At the origin a trivial steady state always exists. It is stable for some values of J and unstable for others thus it is not shown on the figure. Dotted curves mean that the corresponding steady state is unstable, while full curves indicate that the corresponding steady state is stable. For the left column $J \in [0; 4]$, while for the right column $J \in [0; 10]$.

As X_0 and Y_0 are non negative, the minimal, allowed value of z is 1. Expression (34) is negative if and only if

$$z^2 - \alpha z - \alpha > 0 \,. \tag{36}$$

For any $\alpha > 0$ there is exactly one positive solution to $z^2 - \alpha z - \alpha = 0$, being $\frac{1}{2}\left(\alpha + \sqrt{\alpha^2 + 4\alpha}\right)$. Any larger z value fulfills (36) and since $z \geq 1$ is required we get

$$z_{crit} = \max\left\{\frac{1}{2}\left(\alpha + \sqrt{\alpha^2 + 4\alpha}\right), 1\right\}\,. \tag{37}$$

Solving for $X_0 + Y_0$ this implies that the bound M is

$$M = z_{crit}^2 - 1, \tag{38}$$

i.e. for $X_0 + Y_0 > M$ are $X_0' < 0$ and $Y_0' < 0$. Note that we may chose

$$\alpha = \frac{\max\{1, \frac{R}{D_0}\} \cdot \max\{J, \sqrt{2B_x}, \sqrt{2B_y}\}}{\min\{1, C_x, C_y\}}\,. \tag{39}$$

Thus, $M \geq 0$ and the triangle defined by the X_0-axis, the Y_0-axis and the line $X_0 + Y_0 = M$ thus define an attractive trapping region for equation (10). We emphasize that M generally depends on D_0 and J as well as $R, B_x, B_y, C_x,$ and C_y.

4.3. Phase plane analysis and treatments

In the present work we mainly focus on analyzing the impact of the inflammatory stimuli J, modifying the T-cell independent death rate D_0, and modifying the T-cell response represented by D_1 rather than a complete analysis of real treatments. However, several treatment scenarios are possible, e.g. T-cell therapy. Interferon-α treatment among other things stimulates the immune system, whereby the effect of the effector T-cells become strengthened.

The reduced model has been investigated numerically for various choices of parameters. The default parameters, as given in table 2, have been used when nothing else is stated.

First consider the default case $\frac{D_0}{R} < 1$ as illustrated in figure 6 showing the phase plane for various J and D_1. A trivial steady state F_0 is found to always exist, and, for sufficiently low inflammatory stimuli J, it is stable. For J greater than $\frac{D_0}{2R}$, a purely leukemic steady state F_L becomes admissible and the leukemic cells increase in numbers with increasing J. For choices of J where only F_L and F_0 are admissible, the leukemic steady state is found to be stable, whereas the trivial state is unstable. It is worth emphasizing that the purely leukemic steady states in general only depend on the four clusters of parameters $\frac{D_0}{R}, \frac{D_1}{R}, \frac{JR}{D_1}, B_y,$ and J.

For J greater than $\frac{1}{2}$, an unstable hematopoietic steady state, F_{H+}, becomes admissible. In absense of mutations, i.e. no malignant cells present, the hematopoietic steady state appears stable. Being a saddle point with stable manifold along the X_0-axis and the unstable manifold having a non-vanishing Y_0-component, a perturbation with malignant cells may cause the state to be repelling away from the hematopoietic steady state. As was shown analytically, F_{H+} only depends on the two parameters J and B_x and for fixed B_x, X_{0H+} increases with J.

As shown in figure 6, an admissible co-existence steady state, F_C may exist, which is dependent on both J and D_1. While it has been found to exist for sufficiently high J, regardless of realistic values of D_1, the existence of F_C does require very large values of J for $D_1 \leq 0.1$. For default parameter values (e.g. $D_1 = 0.1$) the co-existing steady state occurs for J larger than J_c given by equation (26). The co-existing steady state is stable and bifurcates from the leukemic steady state which loses its stability and becomes unstable. For increasing J, F_C moves away from F_L with increasing X_0. For D_1 around 1 or greater, the co-existence steady state might represent a possible preferable situation to the full-blown leukemic state F_L. For large choices of D_1, such as $D_1 = 10$ shown in figure 6, F_C is in close proximity of F_{H+} for most realistic choices of J, leading to a co-existence steady state, which can be interpreted as having a small number of leukemic cells, which are held back from increasing due to a strong T-cell response. In the case where the co-existence steady state exists, it is found numerically to be stable, while the leukemic steady state F_L becomes unstable whenever the co-existing steady state becomes admissible. Thus, for any situation where a co-existence steady state is admissible, the system will move towards this state.

Increasing B_y, D_0 or D_1 and decreasing R cause the leukemic steady state to appear at higher values of J while increasing B_x causes the hematopoietic steady state to occur for lower values of J. Thus, the model identifies important parameters for potential protection to prevent a leukemic outbreak.

Next, consider the case $\frac{D_0}{R} > 1$ in contrast to the default case. Phase plane portraits are shown in figure 7 for various J and D_0. The situation is analogous to the default case except the order in which the hematopoietic steady state and the leukemic steady state occur are interchanged along with their stability properties. Thus the hematopoietic steady state bifurcates from the trivial steady state and takes over the stability for increasing J shown in the second and third row of figure 7. For larger J-values the leukemic steady state bifurcates from the trivial one as an unstable steady state and it remains unstable for larger J. For even larger values of J the co-existing steady state bifurcates from the hematopoietic steady state and it takes over the stability leaving the hematopoietic steady state unstable.
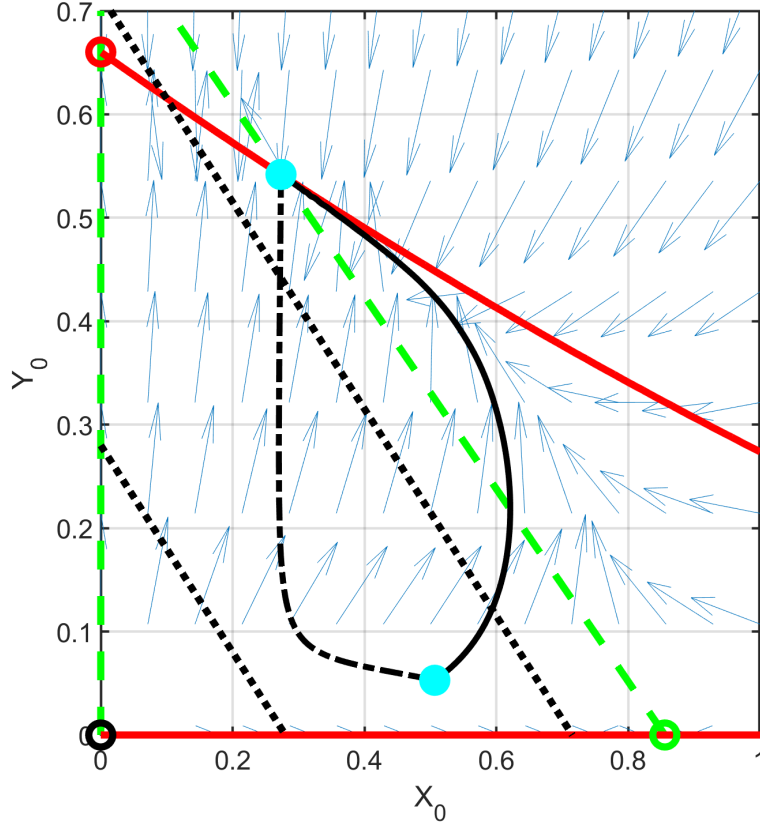
Figure 9: An *in silico* treatment of a virtual patient having (D_1, J)=(1,0.9). The treatment combines gene therapy, by increasing D_1 to 10, and an anti-inflammatory treatment, by lowering J from 0.9 to 0.76. Hereby the virtual patient is moved from a co-existing steady state (upper cyan dot) with high malignant cell counts, (X_0, Y_0)=(0.27,0.55) corresponding to (D_1, J)=(1,0.9), toward a co-existing steady state (lower cyan dot) with low malignant cell count and normalized hematopoietic cell count, (X_0, Y_0)=(0.51,0.05) corresponding to (D_1, J)=(10,0.76). This treatment path (stipulated black curve) do not follow the displayed slope field. Thereafter treatment is put on pause and the virtual patient follows the flow back toward the original co-existing steady state (full black curve), (X_0, Y_0)=(0.27,0.55). Full red lines show the Y_0 nullcline and the stipulated green lines show the X_0 nullcline. The open circles illustrate the unstable steady states (black for the trivial, red for the leukemic, and green for the normal hematopoietic steady state). The black dotted lines bound the region, which represents the total leukocyte count considered to be normal. Above the upper boundary the risk of thrombosis is considered high and below the lower boundary the immune system is considered to be dysfunctional.

For increasing J it slowly moves away from the hematopoietic steady state. Compared to the default case, $\frac{D_0}{R} < 1$, this is not necessarily lethal, since X_{0C} stays relatively close to X_{0H} and $Y_{0C} \ll Y_{0L}$.

Returning to the case $\frac{D_0}{R} < 1$, a scenario of an *in silico* treatment of a virtual patient having $(D_1, J) = (1,0.9)$ is illustrated in figure 9. The treatment combines a strengthened T-cell effect (interferon or T-cell therapy) by increasing D_1 to 10 and an anti-inflammatory treatment, which lowers J from 0.9 to 0.76. Thus, the virtual patient is moved from a co-existing steady state with high malignant cell counts, $(X_0, Y_0)=(0.27,0.55)$ towards a co-existing steady state with low malignant cell counts and normalized hematopoietic cell counts, $(X_0, Y_0)=(0.51,0.05)$. This treatment path (stipulated curve) does not follow the displayed slope field shown, corresponding to $(D_1, J)= (1,0.9)$. It takes approximately 5 years for the treatment to lower Y_0 to 15%, but almost 20 years to increase X_0 to near normal amount. The total cell count $(X_0 + Y_0)$ is fairly well controlled during this treatment process, which is essential to prevent high risk of thrombosis. Thereafter treatment is put on pause and the virtual patient follows the flow back toward the original co-existing steady state, $(X_0, Y_0)=(0.27,0.55)$. It takes about 20 years for Y_0 to pass 0.5 corresponding to 10% below the original amount. The time interval of treatment and relapse are both quite large and it is likely that the malignant cells develop resistance during such time span. On the other hand these time scales are comparable to clinical experiences.

To explicitly include resistance in the model, we assume that the exposure,

$$U = \int_0^t Y_0(t)\, dt, \tag{40}$$

of malignant stem cells drives the development of resistance. Furthermore, we assume that resistance inhibits the Y_0-dependent death rate D_1 by a decreasing Hill-function in the exposure, as it is associated with a reduced T-cell elimination of the malignant cells. Thus, the death rate, D_1, in equation (10b) is substituted by,

$$\frac{D_1}{1 + U^8}. \tag{41}$$

We note that, as exposure increases, the effective death rate in equation (41) decreases, leading to an increase in Y_0, which further increases exposure and so on. Initially, the development will be like that seen for the co-existing steady state (as shown in figure 4 for $D_1 = 5$), but as the exposure increases, resistance develops and the dynamic starts to deviate from that without resistance. Thus, after approaching the co-existing steady state for a while the cancer development begins to increase approximately as an exponential-function (for the second time) before finally reaching the

saturation level, corresponding to full blown cancer, as seen in figure 10. Meanwhile the hematopoietic cells show a reciprocal development. Overall, the co-existing stable steady state is approached in the first phase of the development, while resistance develops. When resistance becomes influential, around year 30, the co-existing steady state disappears and in the next phase the full blown cancer develops. Thus, the developed resistance destroys the effect of the therapy over time. We have chosen the Hill power to be 8 in equation (41). Choosing it larger does not change the numerical output significantly and choosing it smaller makes the dormancy state, i.e. the temporary plateau between year 25 and 40 in figure 10, shorter and resistance will start a bit earlier. For $U = 1$, expression (41) takes the saturation value $\frac{1}{2}D_1$. This half saturation value corresponds approximately to year 42 at figurẽreffig:resistance.
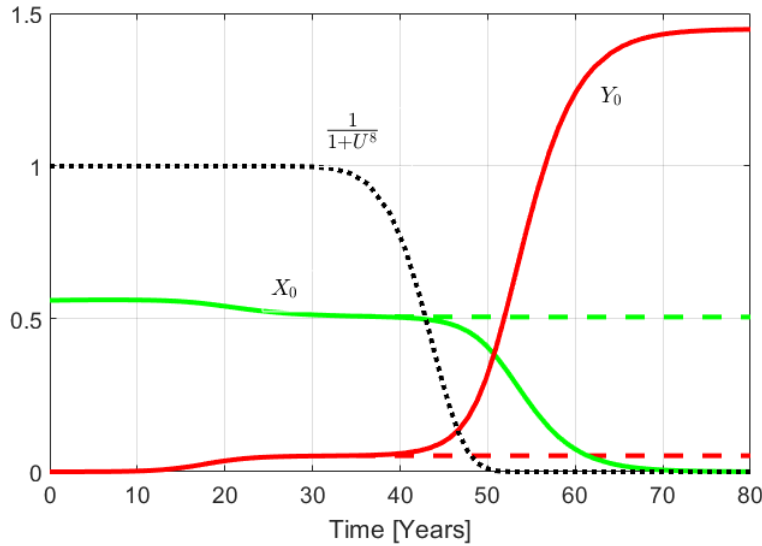

Figure 10: Effects of resistance of malignant stem cells to T-cell elimination. The dotted lines show the cancer development toward the co-existing steady state in absence of resistance whereas the full lines show the development when resistance develops. Green curves represent the hematopoietic stem cell counts (X_0) and the red curves represent the malignant stem cell counts (Y_0). Parameters are as for figure 4 but with $D_1 = 10$. Black dotted line shows the inhibiting factor $\frac{1}{1+U^8}$ over time, reducing the population death due to resistance. All quantities are shown in dimensionless units except time which is in years. See section 5 for further discussion.

A specific finding deserves to be emphasized: A dimensionless stem cell reproduction ratio $\mathcal{R}$ exists, which determines how robust the hematopoietic condition may be and how disastrously a potential blood cancer disease will develop. This is similar to the concept of a reproduction number in epidemiology describing whenever an epidemic outbreak may occur. In our case, the reproduction ratio consists of a combination of six physiological

30

parameters from the dimensional form of the full model. Inspired by the different topologies discussed above, we define the reproduction ratio as the inverse of $\frac{D_0}{R}$,

$$\mathcal{R} = \left(\frac{D_0}{R}\right)^{-1} = \frac{\left(\frac{r_y}{\hat{d}_{y0}+a_y}\right)}{\left(\frac{r_x}{d_{x0}+a_x}\right)} \tag{42}$$

Thus for $\mathcal{R} > 1$ we have a more serious situation than for $\mathcal{R} < 1$, showing that if the reproduction ratio exceeds the threshold $\mathcal{R}_0 = 1$ it is more disastrous than if it is below $\mathcal{R}_0$. Physiologically the reproduction ratio $\mathcal{R}$ tells us that the situation is worse if malignant stem cells have a better fitness than the hematopoietic stem cells. The intuitive interpretation in most biomedical literature attributes the main cause for cancer development to the frequency of stem cell division. Our fitness concept, the ratio between the self-renewal rate and the sum of the death rate and the proliferation rate, is far more nuanced, but is in agreement with the literature and furthermore, which also confirms our results. To force the model from a regime of highly disastrously development into a regime of less disastrously development we may simply focus on how to manipulate the reproduction ratio, $\mathcal{R}$, for the specific system under consideration to become less than the threshold value of $\mathcal{R}$. The threshold concept depends on six parameters, which offer independent manipulation possibilities. Alternatively, one may consider the fitness of hematopoietic cells as a given fitness threshold value for a specific system. Thus the development of a given mutation is determined by the fitness value of that mutation compared to that of the hematopoietic cells.

In addition to the primary reproduction ratio $\mathcal{R}$, a secondary reproduction number, $\mathcal{S}$, important for the dynamics of the system as it appears in most analytical expressions (see Appendix B), is,

$$\mathcal{S} = \left(\frac{D_1}{R}\right)^{-1} = \frac{\left(\frac{r_y c_{yy}}{\overline{y}_0}\right)}{\left(\frac{r_x}{d_{x0}+a_x}\right)}. \tag{43}$$

This secondary reproduction number, $\mathcal{S}$, describes the T-cell dependent fitness of the malignant stem cells relative to the afore defined fitness of the hematopoietic stem cells, whereas the primary reproduction ratio, $\mathcal{R}$, compares the T-cell independent fitness of malignant stem cells to that of hematopoietic stem cells.

Increasing the inflammatory stimuli J accelerates and drives the blood cancer in general. Vice versa, the blood cancer itself induces an inflammatory response, and thus the coupled system introduces a negative spiral with respect to the disease development. For further details on this see [2].

5. Discussion and conclusion

A novel mechanism-based model - the Cancitis model - describing the interaction of blood cancer and the inflammatory system is proposed. The immune response is divided into two components, one where the elimination rate of malignant stem cells is independent of the size of the cancer (Y_0-independent death rate) and one where the elimination rate depends on the size of the cancer (Y_0-dependent death rate). The model confirms that inflammation may accelerate and drive a cancer beyond the fact that the presence of a cancer induces an inflammatory response. A dimensional analysis shows that the full 6-dimensional system of nonlinear ordinary differential equation may be reduced to a 2-dimensional system - the reduced Cancitis model. In terms of Fenichel theory this is known as the reduced model or the slow manifold approximation. This is a very good approximation and is appropriate for MPNs in particular, since these diseases develop slowly. The original parameters appear in the reduced model in clusters, showing the important grouping of parameters. The reduced model allows for a highly analytical investigation of steady states and their dependence especially on the inflammatory stimuli J, the Y_0-independent death rate (D_0) and the Y_0-dependent death rate (D_1). A semi-analytic investigation reveals the stability properties of the steady states. Finally, we prove positivity of the system and the existence of an attracting trapping region in the positive octahedron guaranteeing global existence and uniqueness of solutions. For the reduced Cancitis model the possible topologies are completely described as having a Janus structure, where two qualitatively different topologies appear for different sets of parameters given by $\mathcal{R}$. In the important work by Stiehl et. al. [64] a model without immune interaction is presented. The authors discuss a fraction similar to $\mathcal{R}$ given in equation (42) and shows that it is important for the dynamics of the system. However, this model involved explicitly the hierarchy of progenitor cells, whereby a lot of unknown parameter are introduced, thus their results appear as a more qualitative analysis involving all these parameters. The relative simplicity of our model, due to the parsimonious principle and the model reduction, make it possible to state sharp criteria involving $\mathcal{R}$, which along with another threshold $\mathcal{S}$ given in equation (43) deliver a complete topological analysis of the possible dynamics.

For the default parameters a trivial steady state F_0 always exist. Starting by no stimulation J of the inflammatory system only the trival steady state is stable. Increasing J will turn this trival steady state into an unstable steady state while a leukemic steady state appears. If J is increased further an unstable hematopoietic steady state occurs. In absense of mutations, i.e. no malignant cells, the hematopoietic steady state is stable. Being a saddle point, a pertubation of the hematopoietic steady state with malig-

32

nant cells may cause the state to be repelling away from the hematopoietic steady state. At the bifurcation the purely leukemic steady state takes over the stability turning the trivial steady state into an unstable state. Both the hematopoietic steady state and the leukemic steady state start at the trivial steady state, and move away from it with increasing values of J. A co-existing steady state bifurcates from the leukemic one for even higher values of J and simultaneously the leukemic steady state loses its stability. For increasing values of J, the co-existing steady state moves towards higher X_0-values and with only a minor increase in Y_0. Increasing D_1 also decreases Y_0, thus representing an attractive disease condition compared to full blown blood cancer.

We emphasize that the choice of default parameter values for C_x and C_y make the highest order coefficient in equation (B.23), given in expression (B.24), relatively small, since $C_x C_y \approx 1$. As a consequence not only the roots of equation (B.23), but also the number of real roots become sensitive to these parameter values. Thus some caution is needed; A considerable change in parameters may not only change the stability properties, but also the number of possible co-existing steady states. The outbreak of blood cancer in general is commonly considered to occur when the ratio of the self-renewal rates, R, exceeds a threshold value, frequently taken to be one. However, the model implies that the ratio between R and the cell death rates D_0 and D_1 should rather be considered. In fact, the analysis motivates the definition of a primary and a secondary reproduction ratio, $\mathcal{R}$ and $\mathcal{S}$, respectively, crucially for topology of the dynamics of the system. If $\mathcal{R}$ is larger than one, the leukemic steady state appears first and the hematopoietic steady state later for increasing J. The leukemic steady state is stable until the co-existing steady state may take over. If instead, $\mathcal{R}$ is less than one, the hematopoietic steady state appears first and the leukemic steady state later with respect to increasing J. Thus the hematopoietic steady state is stable until the co-existing steady state takes over while the leukemic steady state remains unstable. Inflammation is presumably another important quantity for the onset and development of blood cancer, greatly influenced by the inflammatory stimulation J [19, 10, 39, 33, 31, 30, 71, 72, 2, 29]. This suggests that the body may manage initial leukemia as long as the self-renewal rate is not too high, but fails to manage it if an inflammation appears. These findings suggest combining treatment with anti-inflammatory treatment. Thus inflammation may trigger and drive blood cancers including MPNs.

It is interesting that decreasing the inflammatory stimuli for $\mathcal{R} > 1$ may not be a good first step in treatment of such patients. Instead D_1 should be increased first and subsequently the inflammatory stimuli may be reduced. However, for $\mathcal{R} < 1$ the inflammatory stimuli may be reduced simultaneously with increasing D_0.

We note that, increasing the inflammatory stimuli (I) increases $J = \frac{I}{2e_s\bar{s}} = I\frac{(r_x/e_s)}{d_{x0}+a_x} = \frac{I}{e_s}\frac{r_x}{d_{x0}+a_x}$. An increase in the rate r_x increases the amount of hematopoietic stem cells, which quickly increases the amount of mature hematopoietic cells, thus leading to an indirect increases of the amount of dying cells (for unchanged values of d_{x0} and a_x). An increase in the amount of dead cells stimulates the inflammation, whereas e_s eliminates the debris of the dead cells. Thus increasing the fraction r_x/e_s eventually increases the inflammation. This may suggest that drugs helping the inflammatory response in eliminating the debris more effectively may decrease J. However, the denominator $d_{x0} + a_x$ denotes the rate at which hematopoietic stem cells are reduced, due to apoptosis and proliferation into progenitor cells. Hence, an increase in either d_{x0} or a_x will decrease J. The reason why is that a decrease in x_0 in the long term leads to a decrease in x_1 and thus a decrease in the amount of dead cells, a, whereby the inflammatory response become less stimulated. Hence, treatment affecting the stem cells by increasing the natural death rate d_{x0} may decrease the inflammatory response and thereby help reduce the cancer. In combination, the competition between self-renewal rate r_x and the elimination of hematopoietic stem cells $d_{x0} + a_x$ is reflected in the ratio $\frac{r_x}{d_{x0}+a_x}$. Likewise, the competition between the inflammatory load I and the elimination rate of debris by the immune response e_s is reflected in the ratio $\frac{I}{e_s}$. Thus increasing these ratios increase J. This is surprising, since intuitively one would guess that treatment should primarily affect the malignant stem cells and leave the normal hematopoietic stem cell as unaffected as possible. Of course, affecting the amount of normal hematopoietic stem cells has other impacts apart from just affecting J, due to the direct competition between the cell types. Increased J also affect the self-renewal rate for the malignant stem cells. Since the stem cell self-renewal is proportional to J in both cases, the malignant cells benefit most, due to an expected higher baseline self-renewal rate of the malignant stem cells r_y than for the normal hematopoietic stem cells r_x.

The specific inclusion of the T-cells in the immune response has its roots in gene therapy and interferon-α treatment. In gene therapy a patients own T-cells are modified outside the body and re-injected to fight the cancer. As shown, it is in principle a very effective instrument, but in practice it has limited function, since cancer cells almost always develop resistance, by modifying the recognizable surface receptors used by the naive T-cells to identify the cancer cells. Without being recognized by naive T-cells, the effector cells will not attack the cancer cells making this defence weak. Interestingly, even if resistance did not occur, the model predicts that T-cell therapy does not cure the patient, but only keeps the cancer in an iron grip at the co-existing steady state securing limited growth of cancer for a while. When resistance occurs the grip loosens and a fatal growth begins

despite continued T-cell therapy as illustrated on figure 10. The fact is that increasing D_1 by a T-cell therapy may turn a full blown leukemic (stable) steady state into a co-existing (stable) steady state or even for high dose therapy into a healthy (stable) hematopoietic steady state temporarily as illustrated in Figure 7. It takes some years (e.g. 5 years) as illustrated in Figure 9. However, without changing the parameters permanently (e.g. D_1) the cancer recurs either because the cancerous stem cells are not completely eradicated or as soon as a new mutation (surviving repair mechanisms) appears. For a supplementary discussion reaching the same conclusion see [47]. However, for the case of all cancerous stem cells to be completely eliminated 20 years of treatment may be needed. In fact, due to the detection limit, one can never be sure that the cancer is completely eradicated. A detection limit of 1% of 10^{10} mature cells (or 10^4 stem cells) corresponds to 10^8 mature cells (or 100 stem cells). Thus, to guarantee an eradication the malignant stem cells requires a detection limit lower than 0.01%. However, T-cell therapy may be suitable in combination with other treatment.

In the groundbreaking work by Kuznetsov et. al. [41, 42] the intrinsic dynamics of the cells themselves was not considered, but was simply taken as logistic growths independent of the other cell types. In contrast to this we describe the common dynamics of all cell types based on the underlying biological mechanisms. We include the effect of cancerous cells on normal cells and vice versa, their interaction with the dead cells, the dead cells interaction with the immune system, the interaction of the immune system with the replication of (living) cells, and specifically the interaction between cancerous cells and the adaptive immune system, mediated by T-cells and other killer cells. In this way the presented model deviates from the general models in [54, 18, 53, 59, 17, 8, 34, 58, 28, 50, 51, 4, 32, 23, 3, 36, 48, 49]. Thus co-existing states are explicitly shown to be possible as it is shown how such states depends on the important parameters, i.e. inflammatory load and the two relevant death rates. It is shown that in case resistance is considered, this co-existing state is merely a dormancy state and ultimately develops into the full blown cancer state. It is interesting that our mechanism-based multi-cell model confirms previous conclusion that immunotherapy does not completely eradicate malignant cells predicted by Kuznetsov et al [41]. This is an important subject as pointed out by [20].

Besides having a strengthening effect on the effector cells, interferon-α also affects other parts of the cancer-immune system in a constructive synergistic way, which may make the treatment even more effective. A full discussion of how various treatments affect blood cancer and treatment optimization will be addressed in subsequent papers.

Appendix A. Dimensionless form of six dimensional model

Formulating equations on dimensionless form may reduce the number of free parameters by grouping the original parameters into clusters of parameters, the dimensionless parameters. Simultaneously the dimensionless form may suggest a model reduction using Fenichel theory from geometric singular perturbation theory [40].

All variables in equation (1) and (2) are scaled by a constant having the unit of the variable, if any, and it is denoted with same symbol as the variable, but with a bar above. Likewise, the corresponding dimensionless variable is denoted with the corresponding capital letter and with index as the original symbol. Thus we put $x_0 = \overline{x}_0 X_0$, $x_1 = \overline{x}_1 X_1$, $y_0 = \overline{y}_0 Y_0$, $y_1 = \overline{y}_1 Y_1$, $a = \overline{a}A$, $s = \overline{s}S$, and $t = \overline{t}T$, with X_0, X_1, Y_0, Y_1, A, S, and T, the dimensionless variables and $\overline{x}_0$, $\overline{x}_1$, $\overline{y}_0$, $\overline{y}_1$, $\overline{a}$, $\overline{s}$, and $\overline{t}$ the scaling constants carrying the dimensions. Hence the extended model of the differential system in (1) and (2) in the new dimensionless variables reads,

$$X_0' = \overline{t}\left(\overline{s}r_x\frac{S}{1 + (c_{xx}\overline{x}_0 X_0 + c_{xy}\overline{y}_0 Y_0)} - d_{x_0} - a_x\right)X_0 \qquad \text{(A.1a)}$$

$$X_1' = \overline{t}\left(\frac{\overline{x}_0}{\overline{x}_1}a_x A_x X_0 - d_{x_1}X_1\right) \qquad \text{(A.1b)}$$

$$Y_0' = \overline{t}\left(\overline{s}r_y\frac{S}{1 + (c_{yx}\overline{x}_0 X_0 + c_{yy}\overline{y}_0 Y_0)} - d_{y_0}(Y_0) - a_y\right)Y_0 \qquad \text{(A.1c)}$$

$$Y_1' = \overline{t}\left(\frac{\overline{y}_0}{\overline{y}_1}a_y A_y Y_0 - d_{y_1}Y_1\right) \qquad \text{(A.1d)}$$

$$A' = \overline{t}\left(d_{x_0}\frac{\overline{x}_0}{\overline{a}}X_0 + d_{y_0}(Y_0)\frac{\overline{y}_0}{\overline{a}}Y_0 + d_{x_1}\frac{\overline{x}_1}{\overline{a}}X_1 + d_{y_1}\frac{\overline{y}_1}{\overline{a}}Y_1 - e_a\overline{s}AS\right) \qquad \text{(A.1e)}$$

$$S' = \overline{t}\left(r_s\frac{\overline{a}}{\overline{s}}A - e_s S + \frac{I}{\overline{s}}\right) \qquad \text{(A.1f)}$$

putting the mutation rate r_m to zero and where $d_{y_0}(Y_0) = \hat{d}_{y0} + \tilde{d}_{y0}\overline{y}_0 \cdot Y_0$. Here prime denote the derivative with respect to the dimensionless time variable T. To simplify the hematopoietic steady state E_{H+} in equation (3),

as much as we can, we choose

$$\overline{s} = \frac{d_{x_0} + a_x}{r_x} \sim 1 \tag{A.2a}$$

$$\overline{a} = \frac{e_s}{r_s}\overline{s} \sim 10^4 \tag{A.2b}$$

$$\overline{x}_0 = \frac{1}{c_{xx}} \sim 10^4 \tag{A.2c}$$

$$\overline{x}_1 = \frac{a_x A_x}{c_{xx} d_{x_1}} \sim 10^{11} \tag{A.2d}$$

$$\overline{y}_0 = \frac{1}{c_{yy}} \sim 10^4 \tag{A.2e}$$

$$\overline{y}_1 = \frac{a_y A_y}{c_{yy} d_{y_1}} \sim 10^{11} \tag{A.2f}$$

$$\overline{t} = \frac{1}{d_{x_0} + a_x} \sim 10^3 \text{ day} \tag{A.2g}$$

where the order is stated after the $\sim$ symbol based on the default parameter values in table 1. These values are in accordance with those reported in the literature where they are estimated to obtain observed cell counts, see [25, 62, 26]. In addition, we have used 700 as a normal number of dead cells. For further details see [2]. Hence, system (A.1) becomes

$$X_0{}' = \left(\frac{S}{1 + (X_0 + \frac{c_{xy}}{c_{yy}}Y_0)} - 1 \right) X_0 \tag{A.3}$$

$$Y_0{}' = \left(\frac{r_y}{r_x}\frac{S}{1 + (\frac{c_{yx}}{c_{xx}}X_0 + Y_0)} - \frac{d_{y_0}(Y_0) + a_y}{d_{x_0} + a_x} \right) Y_0 \tag{A.4}$$

$$\epsilon_1 X_1{}' = (X_0 - X_1) \tag{A.5}$$

$$\epsilon_1 Y_1{}' = \frac{d_{y_1}}{d_{x_1}}(Y_0 - Y_1) \tag{A.6}$$

$$\epsilon_2 S{}' = \left(A - S + \frac{I}{e_s \overline{s}} \right) \tag{A.7}$$

$$\epsilon_2 \epsilon_3 A{}' = (b_{x_0}X_0 + b_{y_0}(Y_0)Y_0 + b_{x_1}X_1 + b_{y_1}Y_1 - AS) \tag{A.8}$$

where $\epsilon_1 = \frac{r_x}{d_{x_1}}\overline{s} \sim 10^{-5}$, $\epsilon_2 = \frac{r_x}{e_s}\overline{s} \sim 10^{-3}$ $\epsilon_3 = \frac{e_s}{e_a \overline{s}} \sim 10^{-10}$, $b_{x_0} = d_{x_0}\frac{\overline{x}_0 \overline{t}}{\overline{s}\overline{a}}\frac{d_{x_0}+a_x}{e_a} \sim 10^{-13}$, $b_{x_1} = d_{x_1}\frac{\overline{x}_1 \overline{t}}{\overline{s}\overline{a}}\frac{d_{x_0}+a_x}{e_a} \sim 10^{-1}$, $b_{y_0} = (\hat{d}_{y_0}+\tilde{d}_{y_0}\overline{y}_0)\frac{\overline{y}_0 \overline{t}}{\overline{s}\overline{a}}\frac{d_{x_0}+a_x}{e_a} \sim 10^{-13}$, and $b_{y_1} = d_{y_1}\frac{\overline{y}_1 \overline{t}}{\overline{s}\overline{a}}\frac{d_{x_0}+a_x}{e_a} \sim 10^{-1}$. In addition $\frac{d_{y_1}}{d_{x_1}} \sim 1$, $\frac{c_{xy}}{c_{yy}} \sim 1$, $\frac{r_y}{r_x} \sim 1$, $\frac{d_{y_0}+a_y}{d_{x_0}+a_x} \sim 1$, and $\frac{1}{e_s \overline{s}} \sim 1^{-1}$.

We emphasize that the dimensionless variable X_0, X_1, Y_0, Y_1, S and A are all of the same order, since each are normalized by their 'maximal carying capacity'.

Appendix A.1. The reduced extended model - the reduced cancitis model

The system is initially close to the unstable hematopoietic steady state and the development of MPNs is slow, thus we are interested in the reduced system. A naive QSSA may be performed but since several time scales are involved one should be careful. By Fenichel theory the equations (A.3-A.8) involving small epsilon terms may be studied in the limit of vanishing left hand sides, whereby we obtain the reduced cancitis model, i.e. the slow manifold approximation. Thus from equation (A.5-A.6) we obtain the algebraic relations,

$$X_1 = X_0, \tag{A.9a}$$

$$Y_1 = Y_0. \tag{A.9b}$$

Using this in equation (A.8) gives

$$\epsilon_4 A' = (2B_x X_0 + 2B_y Y_0 - AS) \tag{A.10a}$$

with $\epsilon_4 = \epsilon_2 \epsilon_3 \sim 10^{-13}$, $2B_x = b_{x_0} + b_{x_1} \approx b_{x_1} \sim 10^{-1}$, and $2B_y = b_{y_0} + b_{y_1} \approx b_{y_1} \sim 10^{-1}$. Thus we will consider B_y to be independent of Y_0 in what follows.

Thus, from equation (A.7) and (A.10a),

$$S = J \pm \sqrt{J^2 + 2B_x X_0 + 2B_y Y_0} \equiv S_{\pm} \tag{A.11}$$

where only S_+ is non-negative allowing us to disregard the possibility of $S = S_-$ in what follows and thus by substituting S_+ from equation (A.11) into the right hand side of equation (A.7) and putting this equal to zero we get,

$$A = \sqrt{J^2 + 2B_x X_0 + 2B_y Y_0} \tag{A.12}$$

which is always non-negative and where $J = \frac{I}{2e_s \bar{s}}$.

Hence, the reduced cancitis model becomes a closed system in X_0 and Y_0,

$$X_0' = \left(\frac{J + \sqrt{J^2 + 2B_x X_0 + 2B_y Y_0}}{1 + X_0 + C_y Y_0} - 1 \right) X_0 \tag{A.13a}$$

$$Y_0' = \left(R \frac{J + \sqrt{J^2 + 2B_x X_0 + 2B_y Y_0}}{1 + C_x X_0 + Y_0} - D_0 - D_1 Y_0 \right) Y_0 \tag{A.13b}$$

where $R = \frac{r_y}{r_x}$, $D_0 = \frac{\hat{d}_{y0} + a_y}{d_{x_0} + a_x}$, $D_1 = \frac{\tilde{d}_{y0} \bar{y}_0}{d_{x_0} + a_x}$, $C_x = \frac{c_{yx}}{c_{xx}}$, and $C_y = \frac{c_{xy}}{c_{yy}}$. The default dimensionless parameter values are listed in table 2 and we note that all values are of order one. Note, the reduced model involves 8 parameters (including J) where D_1 describe the strength of the Y_0 dependent elimination term in dimensionless form. We emphasize the local existence and uniqueness of solution in the non-negative octahedron. Subsequently we will focus on the impact of the dimensionless inflammatory stimuli J.

Appendix B. Derivations of admissible Steady states

From equation (10a) the **hematopoietic steady state** $F_H = (X_0, 0)$ exist if and only if

$$J + \sqrt{J^2 + 2B_x X_0} = 1 + X_0, \tag{B.1}$$

i.e. if and only if

$$\sqrt{J^2 + 2B_x X_0} = X_0 + 1 - J. \tag{B.2}$$

Disregarding the possibility of double roots a solution exist if and only if $J < X_0 + 1$ (which have to be checked subsequently) given by,

$$X_0^2 - 2(J + B_x - 1)X_0 - (2J - 1) = 0, \tag{B.3}$$

i.e.

$$X_0 = (J + B_x - 1) \pm \sqrt{(J + B_x - 1)^2 + (2J - 1)} \tag{B.4a}$$

$$= (J + B_x - 1) \pm \sqrt{(J + B_x)^2 - 2B_x}. \tag{B.4b}$$

These roots are real if and only if $J \geq -B_x + \sqrt{2B_x}$, a trivial statement for $B_x > 2$ or $J > \frac{1}{2}$, which is not the case for the default parameters.

Putting $J_{H,1} = \frac{1}{2}$ and $J_{H,2} = 1 - B_x$ we may rewrite equation (B.3) as,

$$X_0^2 - 2(J - J_2)X_0 - 2(J - J_1) = 0, \tag{B.5a}$$

Applying Descartes' rule of signs gives that $X_{0+} > 0$ if and only if $J > \min\{J_1, J_2\}$ ($= \frac{1}{2}$ for default parameter values) and $X_{0-} > 0$ if and only if $J_2 < J < J_1$, requiring $B_x > \frac{1}{2}$ (which is not the default case).

The earlier condition $J < X_0 + 1$ may be examined and is equivalent to requiring,

$$\mp \sqrt{(J + B_x)^2 - 2B_x} < B_x, \tag{B.6a}$$

which is trivially fulfilled for X_{0+}. For X_{0-}, this gives

$$J < J_0 \equiv -B_x + \sqrt{B_x^2 + 2B_x}, \tag{B.7}$$

since J is restricted to be positive for physiological reasons.

Hence, F_{H+} is admissible if and only if $J > \min\{J_1, J_2\}$ ($= \frac{1}{2}$ for default parameter values) while F_{H-} is admissible if and only if

$$-B_x + \sqrt{2B_x} < J < -B_x + \sqrt{B_x^2 + 2B_x} \tag{B.8a}$$

and

$$1 - B_x < J < \frac{1}{2} \tag{B.9a}$$

i.e. if and only if

$$-B_x + \sqrt{2B_x} < J < \frac{1}{2} \text{ and } B_x > \frac{1}{2}, \tag{B.10a}$$

which is not in accordance with the default parameter values, meaning that in realistic cases only F_{H+} may be admissible.

The **Purely leukemic steady states** are the solutions of $g(Y_0, J) = 0$ with

$$g(Y_0, J) = R\frac{J + \sqrt{J^2 + 2B_y Y_0}}{1 + Y_0} - D_0 - D_1 Y_0, \tag{B.11}$$

where g is increasing with J. Inserting $Y_0 = 0$ give

$$J_{crit} = \frac{1}{2}\frac{D_0}{R}. \tag{B.12}$$

As $g(y, J)$ is increasing in J, $g(0, J) > 0$ for $J > J_{crit}$. For any fixed J, $g(y, J) < 0$ for y sufficiently large. Since g is continuous, the intermediate value theorem ensures that for any fixed $J > J_{crit}$ there exists a y satisfying $g(y, J) = 0$ i.e. a solution exists to (B.11).
Solutions of (B.11) are roots in the fourth order polynomial

$$\alpha_1 Y_0^4 + \alpha_2 Y_0^3 + \alpha_3 Y_0^2 + \alpha_4 Y_0 + \alpha_5 = 0, \tag{B.13}$$

with the constraint

$$\left(\frac{D_0}{R} + \frac{D_1}{R}Y_0\right)(Y_0 + 1) > J, \tag{B.14}$$

where

$$\alpha_1 = \left(\frac{D_1}{R}\right)^2 \tag{B.15a}$$

$$\alpha_2 = 2\frac{D_1}{R}\left(\frac{D_1}{R} + \frac{D_0}{R}\right) \tag{B.15b}$$

$$\alpha_3 = \left(\frac{D_0}{R}\right)^2 + \left(\frac{D_1}{R}\right)^2 + 2\frac{D_1}{R}\left(2\frac{D_0}{R} - J\right) \tag{B.15c}$$

$$\alpha_4 = 2\left(\left(\frac{D_0}{R} - J\right)\left(\frac{D_0}{R} + \frac{D_1}{R}\right) - B_y\right) \tag{B.15d}$$

$$\alpha_5 = \frac{D_0}{R}\left(\frac{D_0}{R} - 2J\right). \tag{B.15e}$$

Note that $\alpha_1 > 0$, $\alpha_2 > 0$. For large J, $\alpha_3, \alpha_4, \alpha_5$ are all negative so by Descartes' rule of sign there is exactly one positive root to the polynomial

in this case showing that a leukemic steady state is inevitable for large inflammatory stimuli J.

Consider now $B_y < \frac{1}{2}\frac{D_0}{R}\left(\frac{D_0}{R} + \frac{D_1}{R}\right)$. The coefficients $\alpha_3, \alpha_4, \alpha_5$ change sign once with increasing J. The root $J_{L,5}$ of $\alpha_5(J)$ being $\frac{1}{2}\frac{D_0}{R}$, is smaller than the root $J_{L,4}$ of $\alpha_4(J)$, which again is smaller than the root $J_{L,3}$ of $\alpha_3(J)$. This implies that as α_5 crosses zero a unique leukemic steady state is generated and it persists for any larger J values as there is exactly one sign change in the coefficients of the polynomial for any $J > \frac{1}{2}\frac{D_0}{R}$. Solving $\alpha_5 = 0$ gives (B.12). Thus the leukemic steady state emerges at $Y_0 = 0$ for $J = J_{crit}$.

For $B_y > \frac{1}{2}\frac{D_0}{R}\left(\frac{D_0}{R} + \frac{D_1}{R}\right)$, then α_3 remains positive for $J > J_{L,4}$ while α_4 and α_5 behave like in the previous case. Contrary to the previous case there exists a J between $J_{L,4}$ and $J_{L,5}$ such that $\alpha_4 < 0$ and $\alpha_5 > 0$. Hence, there are two sign changes in the coefficients of the polynomial, which indicate 0 or 2 roots. As J is increased such that $\alpha_5 < 0$ there is one sign change in the coefficients for all larger values of J.

The criterion $\alpha_5 > 0$ thus guarantees a unique, positive root to (B.13). Since at least one solution to (B.11) exists in this case, the root of the polynomial must satisfy (B.11).

As the polynomial on the left hand side of (B.13) is decreasing in J and the unique root for $J > \frac{1}{2}\frac{D_0}{R}$ occurs with a positive slope, an increase in J must increase the value of the root i.e. $Y_{0L}(J)$ is increasing for any $J > \frac{1}{2}\frac{D_0}{R}$.

Notice, putting $g = 0$ in equation (B.11) is equivalent to equation (B.18) with $X_0 = 0$. Thus the leukemic steady state and the co-existing steady state are equal for $X_0 = 0$. By implicit function theorem it follows that for $Y_0 \geq Y_{0L}$ the derivative of $X_0 = X_0(Y_0)$ with respect to Y_0 is positive corresponding to an increasing steady state trajectory in J.

From equation (10) **co-existing steady states** $F_C = (X_0, Y_0)$ having positive components exist if and only if

$$J + \sqrt{J^2 + 2B_x X_0 + 2B_y Y_0} = 1 + X_0 + C_y Y_0 \tag{B.16}$$

and

$$J + \sqrt{J^2 + 2B_x X_0 + 2B_y Y_0} = (1 + C_x X_0 + Y_0)\left(\frac{D_0}{R} + \frac{D_1}{R}Y_0\right). \tag{B.17}$$

Assuming solutions exist the equations are equivalent to,

$$1 + X_0 + C_y Y_0 = \left(\frac{D_0}{R} + \frac{D_1}{R}Y_0\right)(1 + C_x X_0 + Y_0) \tag{B.18}$$

and

$$\sqrt{J^2 + 2B_x X_0 + 2B_y Y_0} = 1 + X_0 + C_y Y_0 - J. \tag{B.19}$$

Disregarding the possibility of double roots a solution exist if and only if

$$1 + X_0 + C_y Y_0 > J, \tag{B.20}$$

and

$$(1 + C_x X_0 + Y_0)\left(\frac{D_0}{R} + \frac{D_1}{R}Y_0\right) > J, \tag{B.21}$$

which have to be checked subsequently.

Isolating X_0 in (B.18)

$$X_0 = \frac{(1 + Y_0)\left(\frac{D_0}{R} + \frac{D_1}{R}Y_0\right) - C_y Y_0 - 1}{1 - C_x\left(\frac{D_0}{R} + \frac{D_1}{R}Y_0\right)} \tag{B.22}$$

for non-vanishing denominator and substituting it into (B.19) gives the fourth order polynomium in Y_0,

$$\eta_0 Y_0^4 + \eta_1(J - J_{C,1})Y_0^3 + \eta_2(J - J_{C,2})Y_0^2$$
$$+\eta_3(J - J_{C,3})Y_0 + \eta_4(J - J_{C,4}) = 0. \tag{B.23}$$

where

$$\eta_0 = -\left(\frac{D_1}{R}\right)^2 (C_x C_y - 1)^2 \tag{B.24}$$

$$\eta_1 = -2\frac{D_1}{R}\left(C_x\frac{D_1}{R} - C_x^2 C_y\frac{D_1}{R}\right) \tag{B.25}$$

$$\eta_2 = \left((4\frac{D_0 D_1}{R^2}C_y + 2\frac{D_1^2}{R^2})C_x^2\right.$$
$$\left.+(-2\frac{D_1^2}{R^2} - 2\frac{D_1}{R}C_y - 4\frac{D_0 D_1}{R^2})C_x + 2\frac{D_1}{R}\right) \tag{B.26}$$

$$\eta_3 = \left((2C_y\frac{D_0^2}{R^2} + 4\frac{D_0 D_1}{R^2})C_x^2 + (-2C_y\frac{D_0}{R} - 2\frac{D_0^2}{R^2} - 4\frac{D_0 D_1}{R^2})C_x\right.$$
$$\left.+(-2\frac{D_1}{R})C_x + 2\left(\frac{D_0}{R} + \frac{D_1}{R}\right)\right) \tag{B.27}$$

$$\eta_4 = \left((2\frac{D_0^2}{R^2})C_x^2 + (-2\frac{D_0^2}{R^2} - 2\frac{D_0}{R})C_x + 2\frac{D_0}{R}\right) \tag{B.28}$$

and

$$J_{C,1} = \frac{1}{\eta_1} \left(\left(-2C_y^2 \left(\frac{D_0}{R} \right) + B_y \left(\frac{D_1}{R} \right) - 2C_y \left(\frac{D_1}{R} \right) \right) C_x^2 \right.$$
$$\left. + \left(2 \left(\frac{D_1}{R} \right) + 2(2D_0 + D_1)\frac{C_y}{R} - B_x \frac{D_1}{R} \right) C_x + \frac{2}{R}(D_0 + D_1) \right) \qquad \text{(B.29)}$$

$$J_{C,2} = \frac{1}{\eta_2} \left((C_y^2 \left(\frac{D_0}{R} \right)^2 + 2\frac{D_0 D_1}{R^2}(2C_y - B_y) + \frac{D_1^2}{R^2})C_x^2 \right.$$
$$+ \left(\frac{D_1^2}{R^2}(B_x - 2) - 2C_y \frac{D_0^2}{R^2} - \frac{D_1}{R}(C_y B_x - 2B_y) \right) C_x \right)$$
$$+ \frac{1}{\eta_2} \left(\frac{D_0 D_1}{R^2}(2B_x - 4C_y - 4)C_x - \frac{D_1}{R}B_x + 4\frac{D_0 D_1}{R^2} + \frac{1}{R^2}(D_0^2 + D_1^2) \right)$$
$$\text{(B.30)}$$

$$J_{C,3} = \frac{1}{\eta_3} \left(\frac{D_0^2}{R^2}(2C_y - B_y) + 2\frac{D_0 D_1}{R^2} \right) C_x^2$$
$$+ \left(\frac{D_0}{R}(-B_x C_y + 2B_y) - \frac{D_0^2}{R^2}(-B_x + 2C_y + 2) - \frac{D_0 D_1}{R^2}(-2B_x + 4) \right) C_x$$
$$- \frac{1}{\eta_3} \left(\left(\frac{D_1}{R}B_x \right) C_x - \left(\frac{D_0}{R} + \frac{D_1}{R} \right) B_x + B_x C_y - B_y + 2\frac{D_0}{R^2}(D_0 + D_1) \right),$$
$$\text{(B.31)}$$

$$J_{C,4} = \frac{1}{\eta_4} \left(\frac{D_0^2}{R^2}C_x^2 - \left(2\frac{D_0^2}{R^2} + \frac{D_0}{R}B_x - B_x \frac{D_0^2}{R^2} \right) C_x - \frac{D_0}{R}B_x + B_x + \frac{D_0^2}{R^2} \right). \text{(B.32)}$$

For default values of parameters, equation (B.23) becomes

$$8.72 \cdot 10^{-6}Y_0^4 - 3.68 \cdot 10^{-3}(J + 0.61)Y_0^3$$
$$+4.39 \cdot 10^{-2}(J + 1.06)Y_0^2 + (J - 0.71)Y_0 - 4(J - 0.27) = 0. \quad \text{(B.33)}$$

From the default parameters it follows that $J_{C,2} < J_{C,1} < 0 < J_{C,4} < J_{C,3} < J$ and by Descartes' rule of sign there exists one or three positive and real root if and only if $J > J_{C4}$. From numeric considerations it follows that the number of positive Y_0-roots are three. However, two of these cause X_0 to be negative in acordance with equations (B.20-B.21). Thus exactly one co-existing steady state exist.

[1] Abdel-Wahab, O., Manshouri, T., Patel, J., Harris, K., Yao, J., Hedvat, C., Heguy, A., Bueso-Ramos, C., Kantarjian, H., Levine, R. L. and Verstovsek, S. [2010]. Genetic analysis of transforming events that convert chronic myeloproliferative neoplasms to leukemias, *Cancer Research* **70**(2): 447–452.

[2] Andersen, M., Sajid, Z., Pedersen, R., Gudmand-Hoeyer, J Ellervik, C., Skov, V., Kjær, L., Pallisgaard, N., Kruse, T., Thomassen, M., Troelsen, J., Hasselbalch, H. and Ottesen, J. [2017]. Mathematical Modelling as a Proof of Concept for MPNs as a Human Inflammation Model for Cancer Development, *PLoS ONE* **12(8)**: 1–18.

[3] Arciero, J., Jackson, T. and Kirschner, D. [2004]. A mathematical model of tumor-immune evasion and siRNA treatment, *Discrete and continuous dynamical system-series B* **4**(1): 39–58.

[4] Baker, M., Denman-Johnson, B. B. and Owen, M. [2013]. Mathematical modelling of cytokine-mediated inflammation in rheumatoid arthritis, *Mathematical medicine and biology* **30**: 311–337.

[5] Bangsgaard, E., Hjorth, P., Olufsen, M., Mehlsen, J. and Ottesen, J. [2017]. Integrated Inflammatory Stress (ITIS) Model, *Bull Math Biol.* **79**(7): 1487–1509.

[6] Bangsgaard, E. and Ottesen, J. [2017]. Patient specific modeling of the HPA axis related to clinical diagnosis of depression, *Mathematical Biosciences* **287**: 24–35.

[7] Besse, A., GD, C., Bernard, S., Nicolini, F., Levy, D. and Lepoutre, T. [2018]. Stability analysis of a model of interaction between the immune system and cancer cells in chronic myelogenous leukemia, *Bull. Math. Biol.* **80**: 1084–1110.

[8] Borges, F., Iarosz, K., Ren, H., Batista, A., Baptista, M., Vianna, R., Lopes, S. and Grebogi, C. [2014]. Model for tumor growth with treatment by continuous pulsed chemotherapy., *Biosystems* **116**: 43–48.

[9] Brady, R., Frank-Ito, D., Tran, H., Janum, S., Møller, K., Brix, S., Ottesen, J., Mehlsen, J. and Olufsen, M. [n.d.]. *Mathematical Modelling of Natural Phenomena (In process)* .

[10] Brianna M. Craver, B., Alaoui, K., Scherber, R. and Fleischman, A. [2018]. The critical role of inflammation in the pathogenesis and progression of myeloid malignancies., *Cancers* **10(4)**: 1–18.

44

[11] Campbell, P. and Green, A. [2006]. The myeloproliferative disorders, *N Engl J Med* **355**: 2452–2466.

[12] Cavaillon, J. M. [1994]. Cytokines and macrophages, *Biomed & Pharmacother* **48**: 445–453.

[13] Chen, S.-Y., Huang, Y.-C., Liu, S.-P., Tsai, F.-J., Shyu, W.-C. and Lin, S.-Z. [2011]. An overview of concepts for cancer stem cells, *Cell Transplantation* **20**(1): 113–120.

[14] Chow, C. C., Clermont, G., Kumar, R., Lagoa, C., Tawadrous, Z., Gallo, D., Betten, B., Bartels, J., Constantine, G., Fink, M. P., Billiar, T. R. and Vodovotz, Y. [2005]. The acute inflammatory response in diverse shock states, *SHOCK* **24**(1): 74–84.

[15] Clapp, G., Lepoutre, T., El Cheikh, R., Bernard, S., Ruby, J., Labussire-Wallet, H., Nicolini, F. and Levy, D. [2015]. Implication of autologousimmune system in bcr-abl transcript variations in chronic myelogenous leukemia patients treated with imatinib, *Cancer Research* **75(19)**: 4053–4062.

[16] Clodi, M., Vila, G., Geyeregger, R., Riedl, M., Stulnig, T. M., Struck, J., Luger, T. A. and Luger, A. [2008]. Oxytocin alleviates the neuroendocrine and cytokine response to bacterial endotoxin in healthy men, *Am. J. Physiol. Endocrinol. Metab.* **295**: 686–691.

[17] Cosentino and Bates [2012]. *Feedback control in system biology*, CRC press.

[18] De Pillis, L. G., Radunskaya, A. E. and Wiseman, C. L. [2005]. A validated mathematical model of cell-mediated immune response to tumor growth, *Cancer Research* **65**(17): 7950–7958.

[19] Desterke, C., Martinaud, C., Ruzehaji, N. and Le Bousse-Kerdilés, M. C. [2015]. Inflammation as a keystone of bone marrow stroma alterations in primary myelofibrosis, *Mediators of Inflammation* **2015**: pp.16.

[20] Dingli, D. and Michor, F. [2006]. Successful Therapy Must Eradicate Cancer Stem Cells, *Stem Cells* **24**(12): 2603–2610.
URL: *http://doi.wiley.com/10.1634/stemcells.2006-0136*

[21] Dingli, D., Traulsen, A. and Michor, F. L. [2007]. (a)symmetric stem cell replication and cancer, *PLoS Computational Biology* .
URL: *http://www.ncbi.nlm.nih.gov/pmc/articles/PMC1828703/pdf/*

[22] Dong, Y., Miyazaki, R. and Takeuchi, Y. [2014]. Mathematical modeling on helper t cells in a tumor immune system, *Discrete Continuous Dyn. Syst. Series B* **19**: 55–71.

[23] Dunster, J., HM, B. and King, J. [2014]. The resolution of inflammation: A mathematical model of neutrophil and macrophage interactions, *Bulleting of mathematical biology* **76**: 1953–1980.

[24] Flå, T., Rupp, F. and Woywod, C. [2015]. Bifurcation patterns in generalized models for the dynamics of normal and leukemic stem cells with signaling, *Mathematical Methods in the Applied Sciences* **38**(16): 3392–3407.

[25] Gentry, S. N. and Jackson, T. L. [2013]. A mathematical model of cancer stem cell driven tumor initiation: implications of niche size and loss of homeostatic regulatory mechanisms., *PloS one* **8**(8): e71128.

[26] Haeno, H., Levine, R. L., Gilliland, D. G. and Michor, F. [2009a]. A progenitor cell origin of myeloid malignancies., *Proceedings of the National Academy of Sciences of the United States of America* **106**: 16616–16621.

[27] Haeno, H., Levine, R. L., Gilliland, D. G. and Michor, F. [2009b]. A progenitor cell origin of myeloid malignancies - SUPORTING INFO, *PNAS* (i).

[28] Hanson, S., Grimes, D., Taylor-King, J., Bauer, B., Warman, P., Frankenstein, Z., Kaznatcheev, A., Bonassar, M., Cannataro, V., Motawe, Z., Lima, E., Kim, S., Davila, M. and Araujo, A. [n.d.]. Toxicity Management in CAR T cell therapy for B-ALL: Mathematical modelling as a new avenue for improvement.

[29] Hasselbalch, H. [2012]. Perspectives on chronic inflammation in essential thrombocythemia, polycythemia vera, and myelofibrosis: is chronic inflammation a trigger and driver of clonal evolution and development of accelerated atherosclerosis and second cancer?, *Blood* **119**: 3219–3225.

[30] Hasselbalch, H. [2014]. A role of nf-e2 in chronic inflammation and clonal evolution in essential thrombocythemia, polycythemia vera and myelofibrosis?, *Leukemia Research* **38(2)**: 263–266.

[31] Hasselbalch, H. and Bjoern, M. [2015]. Mpns as inflammatory diseases: The evidence, consequences, and perspectives, *Mediators of Inflammation* pp. 1–16.

[32] Herald, M. [2010]. General model of inflammation, *Bulletin of mathematical biology* **72**: 765–779.

[33] Hermouet, S., Bigot-Corbel, E. and Gardie, B. [2015]. Pathogenesis of myeloproliferative neoplasms: Role and mechanisms of chronic inflammation, *Mediators of Inflammation* pp. 1–16.

[34] Katak, S. [2014]. Mathematical modeling and analysis of tumor-immune system interaction by using Lokta-Volterra predator-prey like model with piecewise constant arguments, *Periodicals of ingineering and natural science* **2**(1): 7–12.

[35] Kim, P., Lee, P. and Levy, D. [2008]. Dynamics and potential impact of the immune response to chronic myelogenous leukemia, *PLoS Comput Biol* **4(6)**: e1000095.

[36] Kirschner, D. and Panette, J. [1998]. Modeling immunotherapy of tumor-immune interaction, *Journal of mathematical biology* **37**: 235–252.

[37] Komarova, N. and Wodarz, D. [2007]. Effect of cellular quiescence on the success of targeted cml therapy, *PLoS one* **48**: e990.

[38] Komarova, N. and Wodarz, D. [2014]. Birkhuser Basel, Springer Science+Business Media New York.

[39] Koschmieder, S., Mughal, T., Hasselbalch, H., Barosi, G., Valent, P., Kiladjian, J.-J., Jeryczynski, G., Gisslinger, H., Jutzi, J., Pahl, J., Hehlmann, R., Vannucchi, A., Cervantes, F., Silver, R. and Barbui, T. [2016]. Myeloproliferative neoplasms and inflammation: whether to target the malignant clone or the inflammatory process or both, *Leukemia* **30(5)**: 1018–24.

[40] Kuehn, C. [2015]. *General Fenichel Theory*, Vol. 191.

[41] Kuznetsov, V. and Knott, C. [2001]. Moddeling tumor regrowth and immunotherapy, *Mathematical and Computer Modelling* **33**: 1275–1297.

[42] Kuznetsov, V. and Makalin, I. [1994]. Nonlinear dynamics of immunogenic tumors: Parameter estimation and global bifurcation analysis, *Bulletin of Mathematical Biology* **56(2)**: 295–321.

[43] Lamond, A. [2002]. Vol. 417 (6887), Garland Science, New York.

[44] Larsen, T., Pallisgaard, N., Mœller, M. and Hasselbalch, H. [2007]. The jak2 v617f allele burden in essential thrombocythemia, polycythemia vera and primary myelofibrosis–impact on disease phenotype, *Eur J Haematol* **79(6)**: 508–515.

[45] McComb, S., Thiriot, A., Krishnan, L. and Stark, F. [2013]. *Introduction to the Immune System*, Vol. 1061, Humana Press, Totowa, NJ.

[46] Michor, F., Hughes, P., T., Iwasa, Y., Branford, S., Shah, N. P., Sawyers, C. L. and Nowak, M. A. [2005]. Dynamics of chronic myeloid leukaemia, *Nature* **435**(7046): 1267–1270.
URL: *http://www.nature.com/doifinder/10.1038/nature03669*

[47] Michor, F., Iwasa, Y. and MA., N. [2006]. The age incidence of chronic myeloid leukemia can be explained by a one-mutation model, *Proc Natl Acad Sci USA* **103**: 14931–14934.

[48] Moore, H. and Li, N. [2004]. A mathematical model for chronic myelogenous luekemia (CML) and T cell interaction, *J theo. Biol.* **227**: 513–523.

[49] Nanda, S., Moore, H. and Lenhart, S. [2007]. Optimal control of treatment in a mathematical model of chronic myelogenous leukemia, *Mathematical Biosciences* **210**: 143–156.

[50] Nielsen, K. H. [n.d.]. *Using Mathematical Modeling to Explore Glucotoxicity as a Precipitating Factor in Type 1 Diabetes as well as a Cause of Low-Grade Autoinflammation in Type 2 Diabetes Hyperglycemia as a Trigger for Autoimmune Diabetes*, PhD thesis.

[51] Nielsen, K. H., Ottesen, J. T. and Pociot, F. [2013]. *Using Mathematical Modeling to Explore Glucotoxicity as a Precipitating Factor in Type 1 Diabetes as well as a Cause of Low-Grade Autoinflammation in Type 2 Diabetes Hyperglycemia as a Trigger for Autoimmune Diabetes*, PhD thesis.

[52] Parish, C. [2003]. Cancer immunotherapy: the past, the present and the future., *Immunol. Cell Biol.* **81**: 106–113.

[53] Pillis, L., Gu, W. and Radunskaya [2006]. Mixed immunotherapy and chemotherapy of tumors: modeling applications and biological interpretations, *Journal of Theoretical Biology* **238**: 841–862.

[54] Pillis, L. and Radunskaya, A. [2003]. The dynamics of an optimal controlled tumor model: a case study., *Mathematical and Computer Modelling* **37**: 1221–1244.

[55] Ribatti, D. [2017]. The concept of immune surveillance against tumors: The first theories, *Oncotarget* **8**(4): 7175–7180.

[56] Robinson, C. [1999]. *Dynamical systems, stability, symbolic dynamics, and chaos*, Studies in advanced mathematics, 2. ed. edn, CRC Press, Boca Raton, Fla.

[57] Roeder, I., Horn, M., Glauche, Hochhaus, A., Mueller, M. and Loeffler, M. [2006]. Dynamic modeling of imatinib treated chronic myeloid leukemia: functional insights and clinical implications, *Nat Med* **12(10)**: 1181–1184.

[58] Saleem, M. and Agrawal [2012]. Complex dynamics in a mathematical model of tumor growth with time delays in cell proliferation, *International Journal of Scientific and Research Publications* **2**(6): 1–7.

[59] Sarkar, R. and Banerjee [2005]. Cancer self remission and tumor stability – a stochastic approach, *Mathematical Biosciences* **196**: 65–81.

[60] Smyth, M., Godfrey, D. and Trapani, J. [2001]. A fresh look at tumor immunosurveillance and immunotherapy., *Nat. Immunol.* **2**: 293–299.

[61] Spivak, J. [2017]. Myeloproliferative Neoplasms, *N Engl Med* **376**(22): 2168–2181.

[62] Stiehl, T., Baran, N., Ho, A. D. and Marciniak-Czochra, A. [2015]. Cell Division Patterns in Acute Myeloid Leukemia Stem-like Cells Determine Clinical Course: A Model to Predict Patient Survival, *Cancer Research* **75**(6): 940–949.

[63] Stiehl, T., Lutz, C. and Marciniak-Czochra, A. [2016]. Emergence of heterogeneity in acute leukemias, *Biology Direct* **11(51)**: 1–19.

[64] Stiehl, T. and Marciniak-Czochra, A. [2012]. Mathematical modeling of leukemogenesis and cancer stem cell dynamics, *Math. Model. Nat. Phenom.* **7**(1): 166–202.

[65] Talkington A, Dantoin, C. and Durrett, R. [2018]. Ordinary differential equation models for adaptive immunotherapy, *Bull. Math. Biol.* **80**: 1059–1083.

[66] Tefferi, A., Vaidya, R., Caramazza, D., Finke, C., Lasho, T. and Pardanani, A. [2011]. Circulating interleukin (il)-8, il-2r, il-12, and il-15 levels are independently prognostic in primary myelofibrosis: a comprehensive cytokine profiling study, *J Clin Oncol* **29**: 1356–1363.

[67] Vaidya, R., Gangat, N., Jimma, T., Finke, C. M., Lasho, T. L., Pardanani, A. and Tefferi, A. [2012]. Plasma cytokines in polycythemia vera: Phenotypic correlates, prognostic relevance, and comparison with myelofibrosis, *American Journal of Hematology* **87**(11): 1003–1005.

[68] Voit, E. [2013]. *A first course in system biology*, Garland Science, Taylor & Francis Group, New York and London.

[69] Walenda, T., Stiehl, T., Braun, H., Fröbel, J., Ho, A. D., Schroeder, T., Goecke, T. W., Rath, B., Germing, U., Marciniak-Czochra, A. and Wagner, W. [2014]. Feedback Signals in Myelodysplastic Syndromes: Increased Self-Renewal of the Malignant Clone Suppresses Normal Hematopoiesis, *PLoS Computational Biology* .

[70] Wilkie, K. [2013]. *Systems Biology of Tumor Dormancy. Chapter 10. A review of mathematical models of cancer-immune interactions in the context of tumor dormancy*, Vol. 734, Springer-Verlag, New York.

[71] Wodarz, D. and Komarova, N. [2014]. World Scientific Publishing.

[72] Zhang, J., Fleischman, A. G., Wodarz, D. and Komarova, N. L. [2017]. Determining the role of inflammation in the selection of JAK2 mutant cells in myeloproliferative neoplasms, *Journal of Theoretical Biology* .